

# Simulations on binary neutron stars: results, difficulties and prospects

Luciano Rezzolla



Albert Einstein Institute, Potsdam, Germany

Dept. of Physics and Astronomy, Louisiana State Univ. Louisiana, USA



Micra2009, Copenhagen, 24-28 August 2009

# Punchline

This is a problem worth attacking.  
Indeed, it that shows all its worth by  
attacking back...



## Plan of the talk

- What we believe is **robust** in the inspiral-merger of:
  - equal-mass, unmagnetized BNSs
  - unequal-mass, unmagnetized BNSs
  - equal-mass, magnetized BNSs
- What we believe is **problematic** in the:
  - postmerger physics and numerics
- What is in our **future workplan** in terms of:
  - improved microphysics and numerics

## Our strengths:

- High-order (up to 8th) finite-difference techniques for the field equations.
- Flux conservative form of HD and MHD equations with constraint transport or hyperbolic divergence-cleaning for the magnetic field; HRSC methods
- Multiple options for the wave extraction (Weyl scalars, gauge-invariant pertbs)
- AMR with moving grids
- Accurate measurements of BH properties through apparent horizons (IH)
- Use excision (matter and/or fields) if needed; good gauges do most of the work

## Our weaknesses:


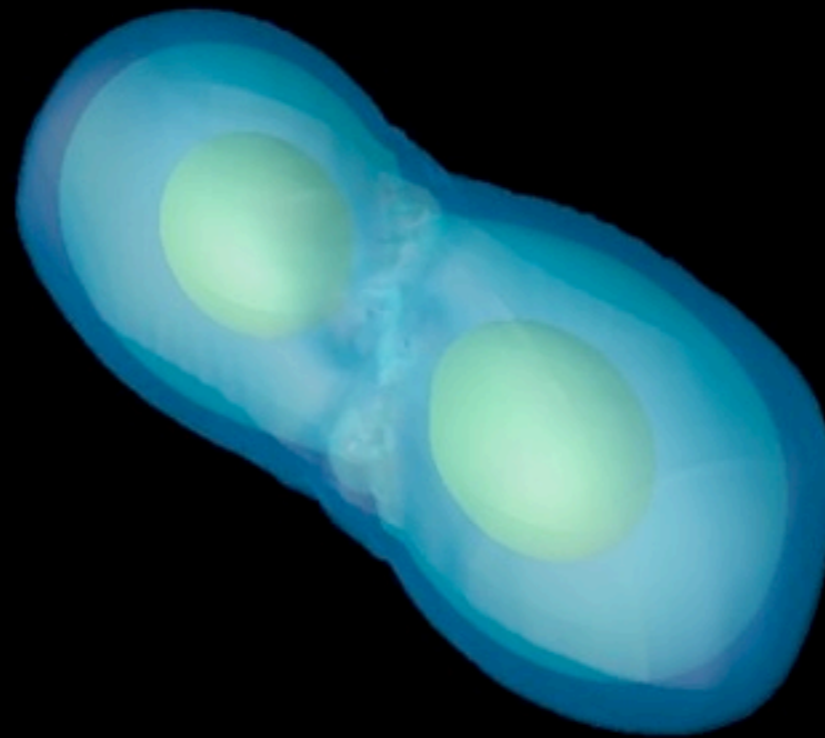
- Idealized (analytic) EOSs (realistic EOSs are implemented but not yet used)
- Single-fluid description: no superfluids nor crusts
- Ideal-MHD: no resistive effects included (work in progress)
- Only inviscid fluid so far (not necessarily bad approximation)
- Radiation and neutrino transport totally neglected (work in progress)
- Match with astrophysical observations inexistent.
- Very coarse resolution; far from regimes where turbulence/dynamos develop

# Unmagnetized **equal**-mass binaries

Baiotti, Giacomazzo, Rezzolla, PRD, 2008

Time=6.250 ms

rest-mass density ( $10^{14}$  g/cm<sup>3</sup>)

A vertical color scale bar ranging from 0 to 6. The colors transition from dark blue at 0, through cyan, green, yellow, and orange, to red at 6.

# Cold vs Hot EOSs

Simplest example of a **“cold”** EOS is the **polytropic** EOS. This **isentropic**: internal energy (temperature) increases/decreases only by mechanical work (compression/expansion)

$$p = K \rho^\Gamma, \quad \epsilon = \frac{K \rho^{\Gamma-1}}{\Gamma - 1}$$

Simplest example of a **“hot”** EOS is the **ideal-fluid** EOS. This **non-isentropic** in presence of shocks: internal energy (i.e. temperature) can increase via shock heating.

$$p = \rho \epsilon (\Gamma - 1), \quad \partial_t \epsilon = \dots$$

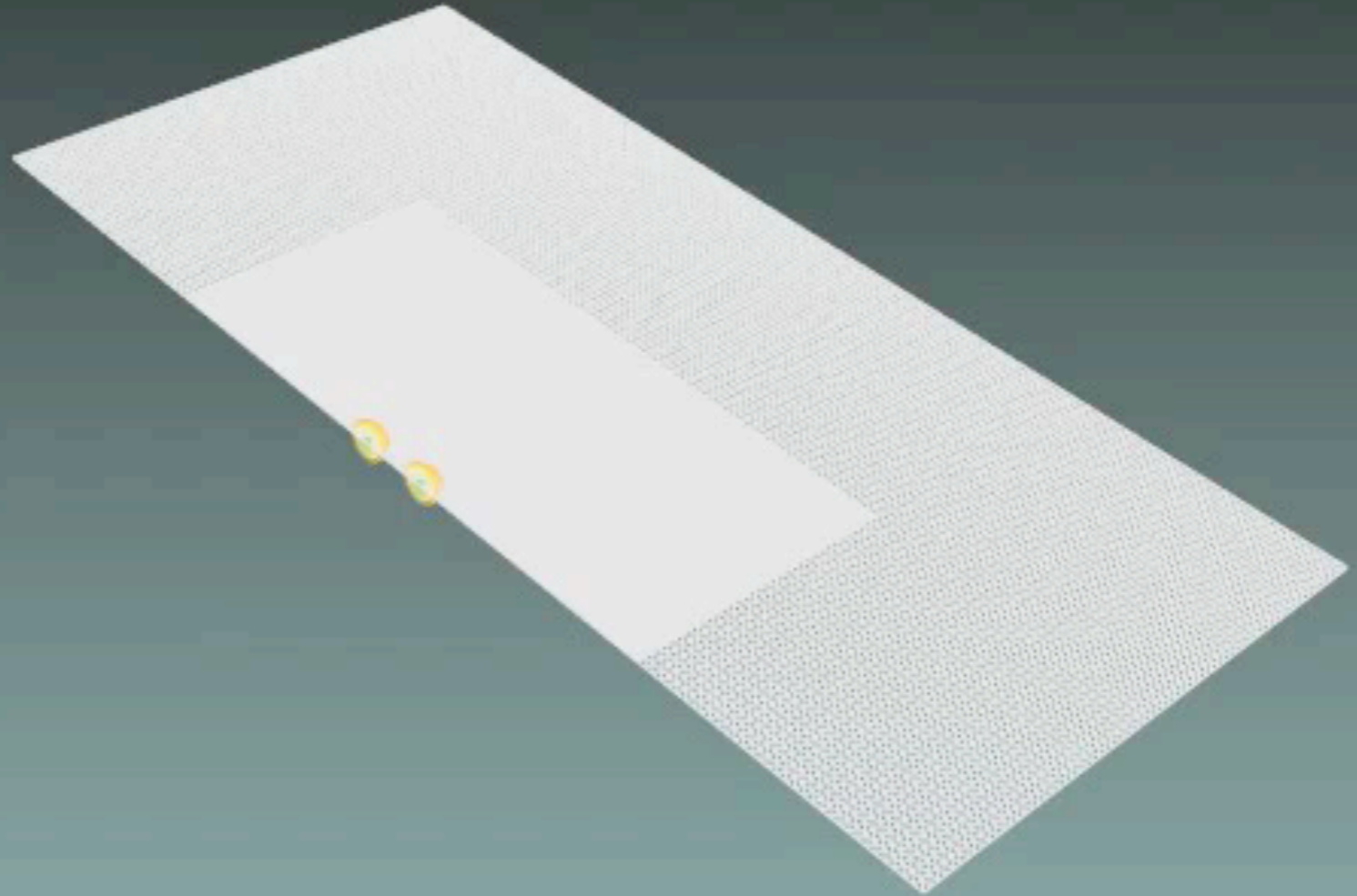
Although analytic, a “hot” EOS is closer much closer to reality but a “cold” EOS is better suited for the inspiral.

Animations: Kaehler, Giacomazzo, Rezzolla

$T[\text{ms}] = 0.00$



$T[M] = 0.00$



Polytropic EOS: high-mass binary

$$M = 1.6 M_{\odot}$$

0.0

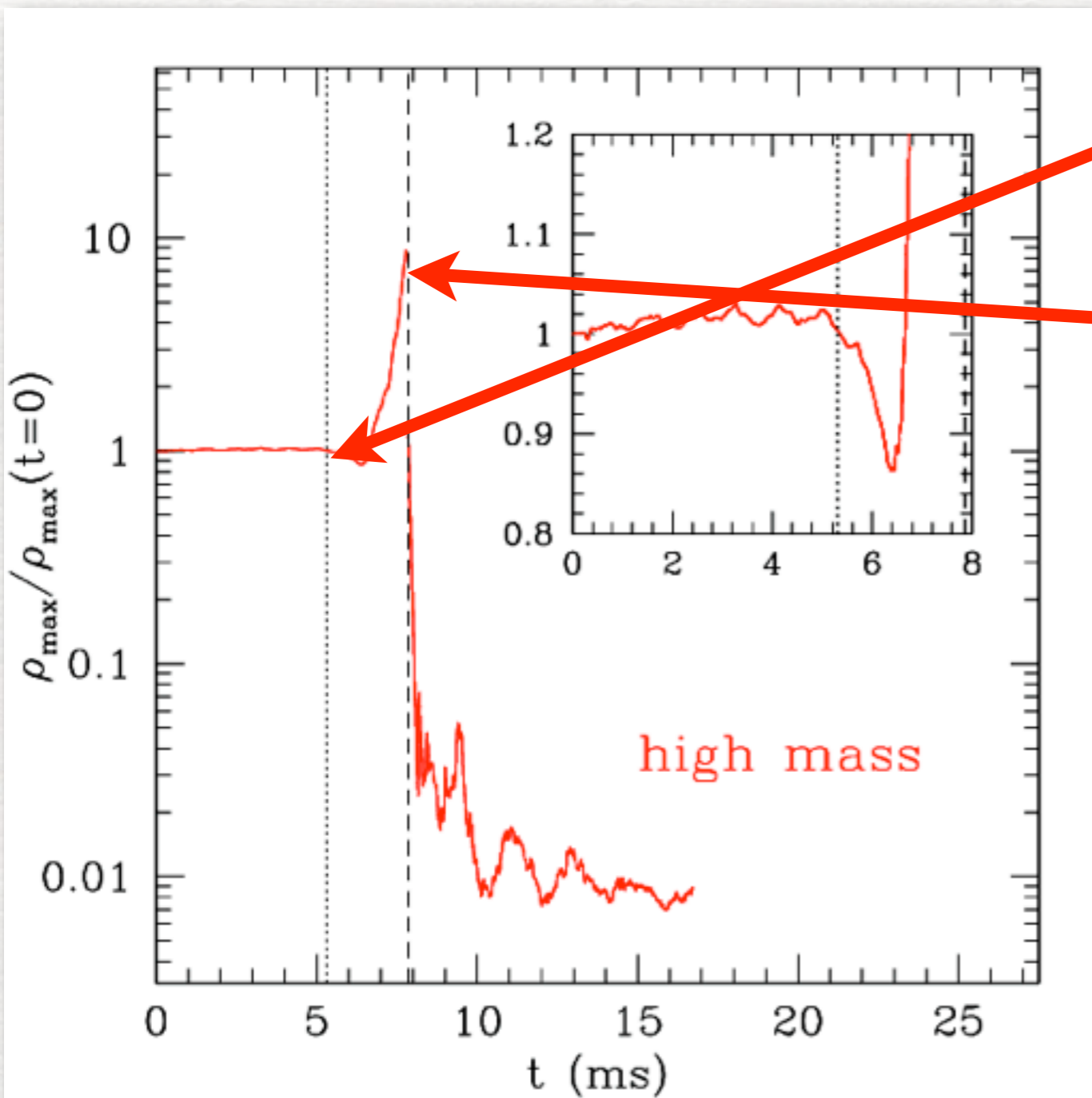
$6.1E+14$



Density [ $\text{g}/\text{cm}^3$ ]

# Matter dynamics

high-mass binary



Merger

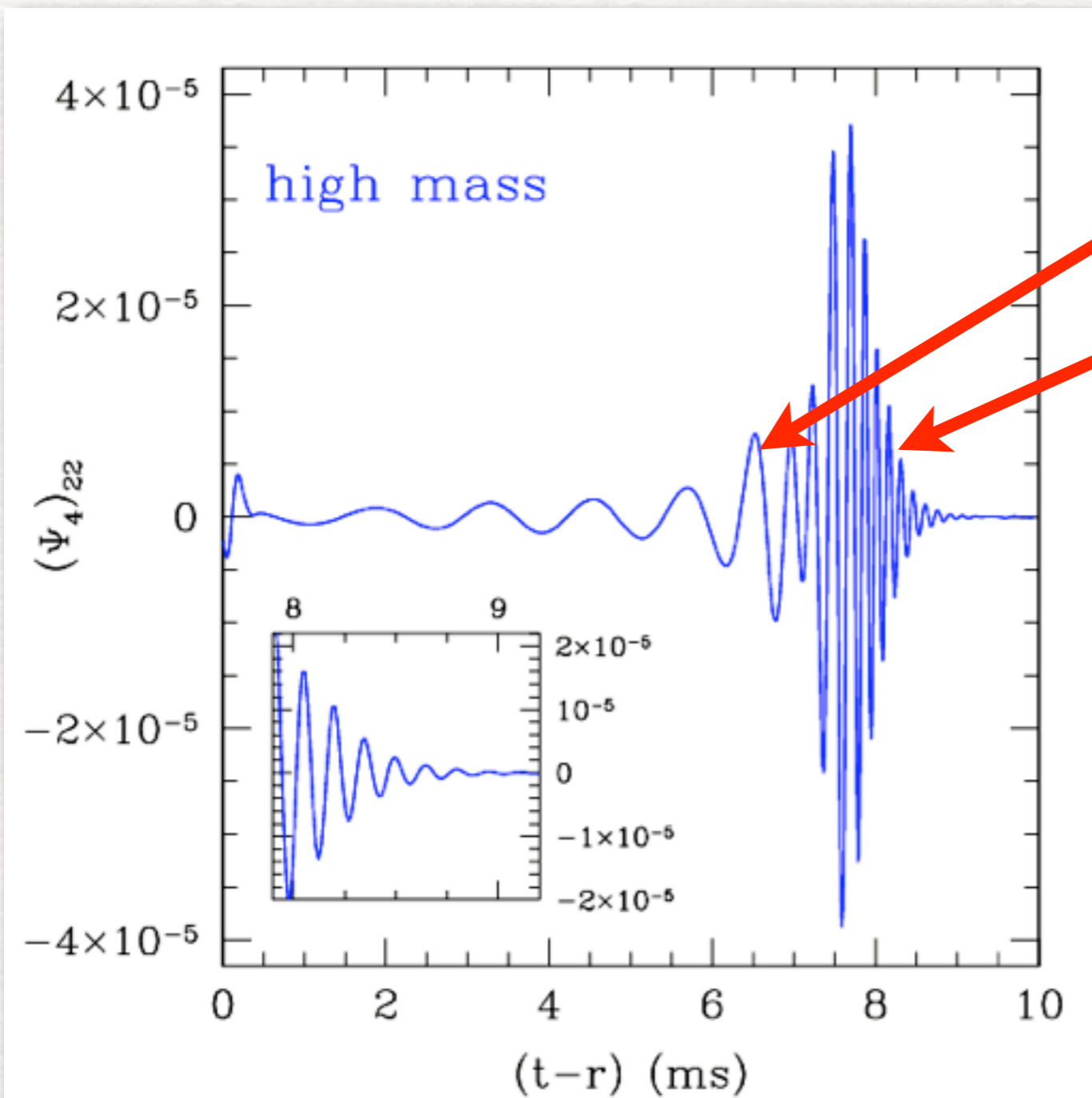
Collapse to  
BH

soon after the merge the torus is formed and undergoes oscillations



# Waveforms: polytropic EOS

high-mass binary



Merger

Collapse  
to BH

first time the full signal from the formation to a bh has been computed

As in CCSNe, we know what to expect:

*“merger → HMNS → BH + torus”*

this behaviour is general but only **qualitatively**

**Quantitative** differences are produced by:

- **differences in the mass for the same EOS:**

a binary with smaller mass will produce a HMNS which is further away from the stability threshold and will collapse at a later time

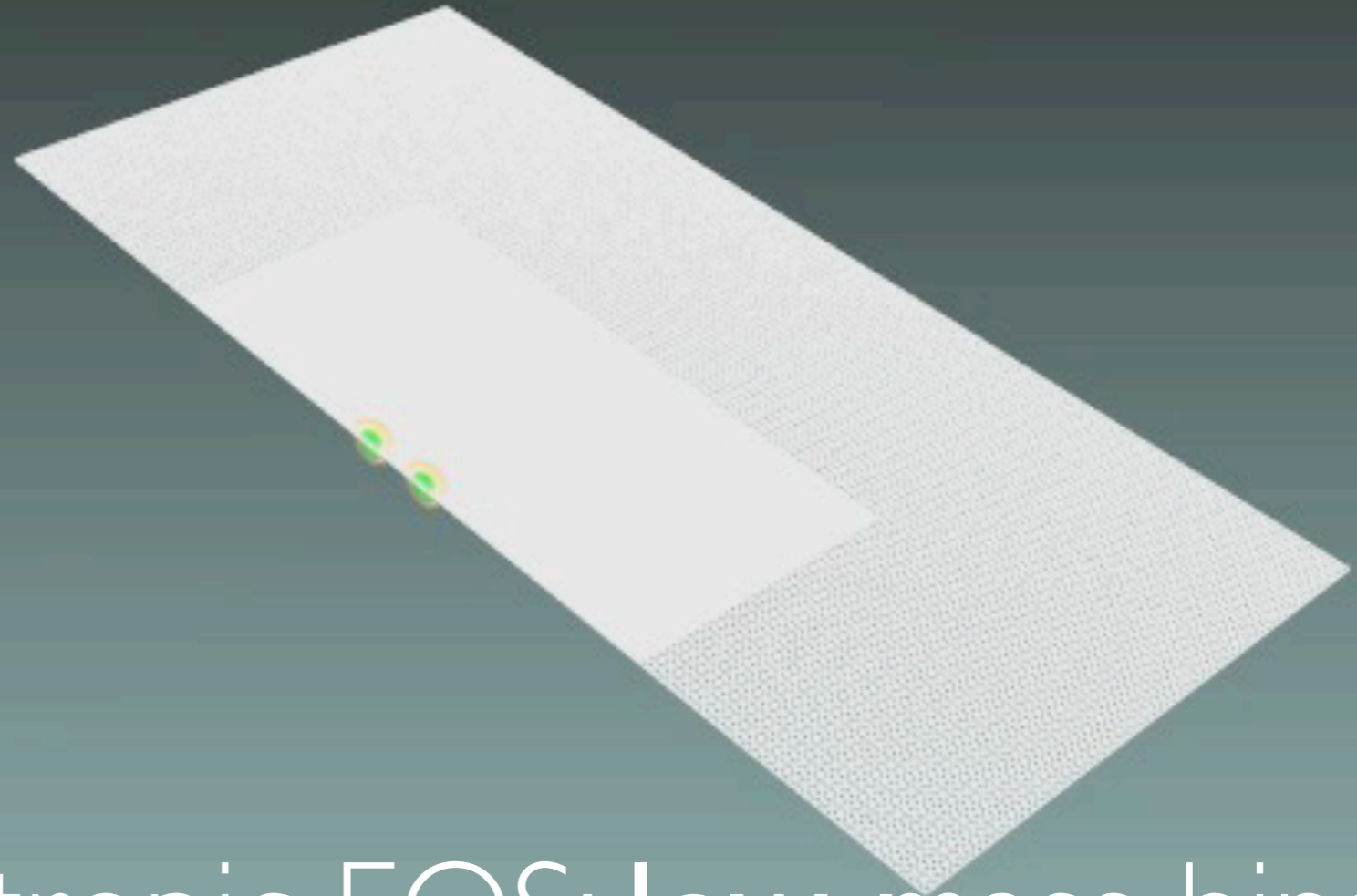
- **differences in the EOS for the same mass:**

a binary with an EOS allowing for a larger thermal internal energy (ie hotter after merger) will have an increased pressure support and will collapse at a later time

$T[\text{ms}] = 0.00$



$T[M] = 0.00$



# Polytropic EOS: **low-mass** binary

$$M = 1.4 M_{\odot}$$

0.0

$6.1E+14$

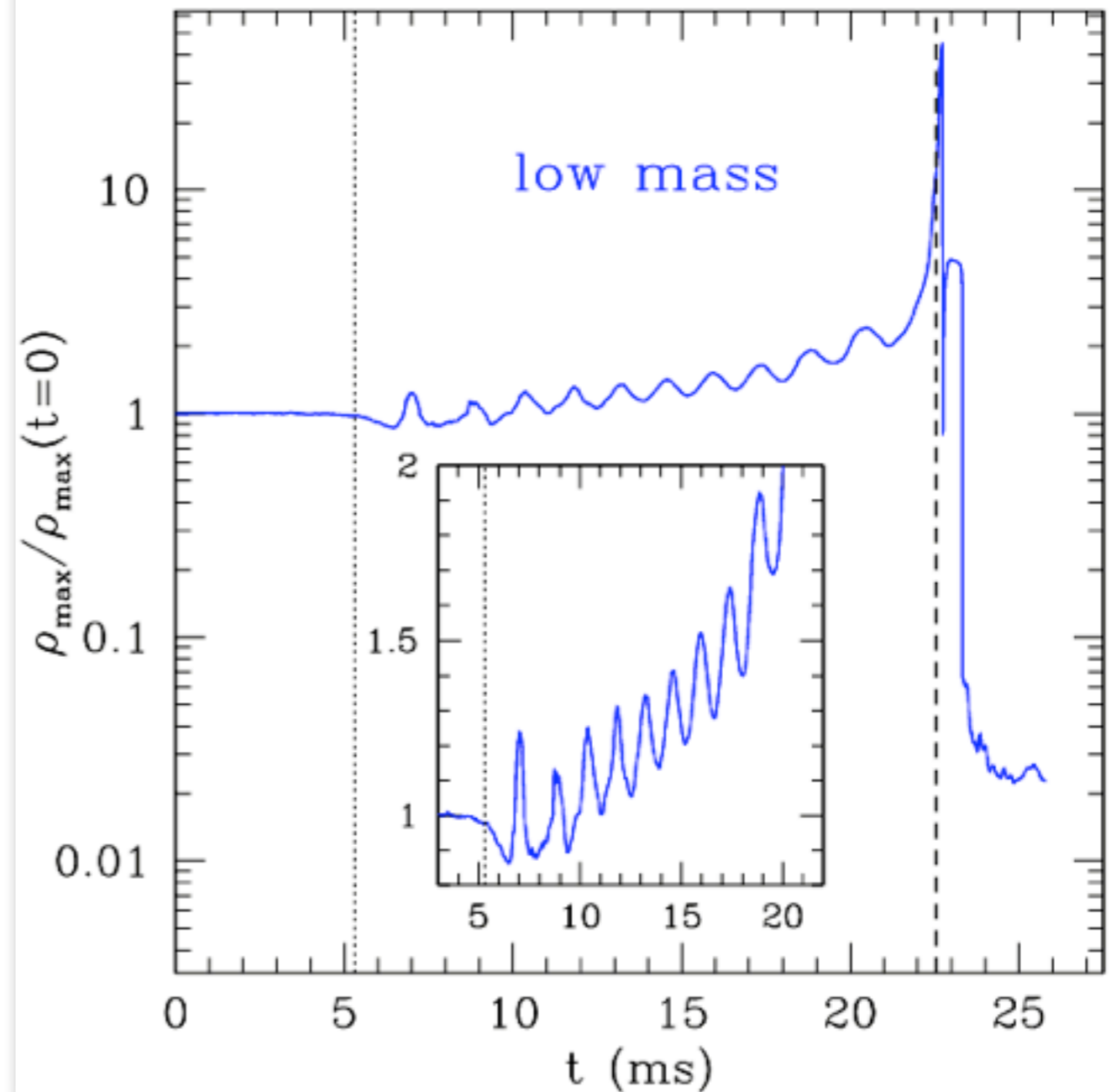
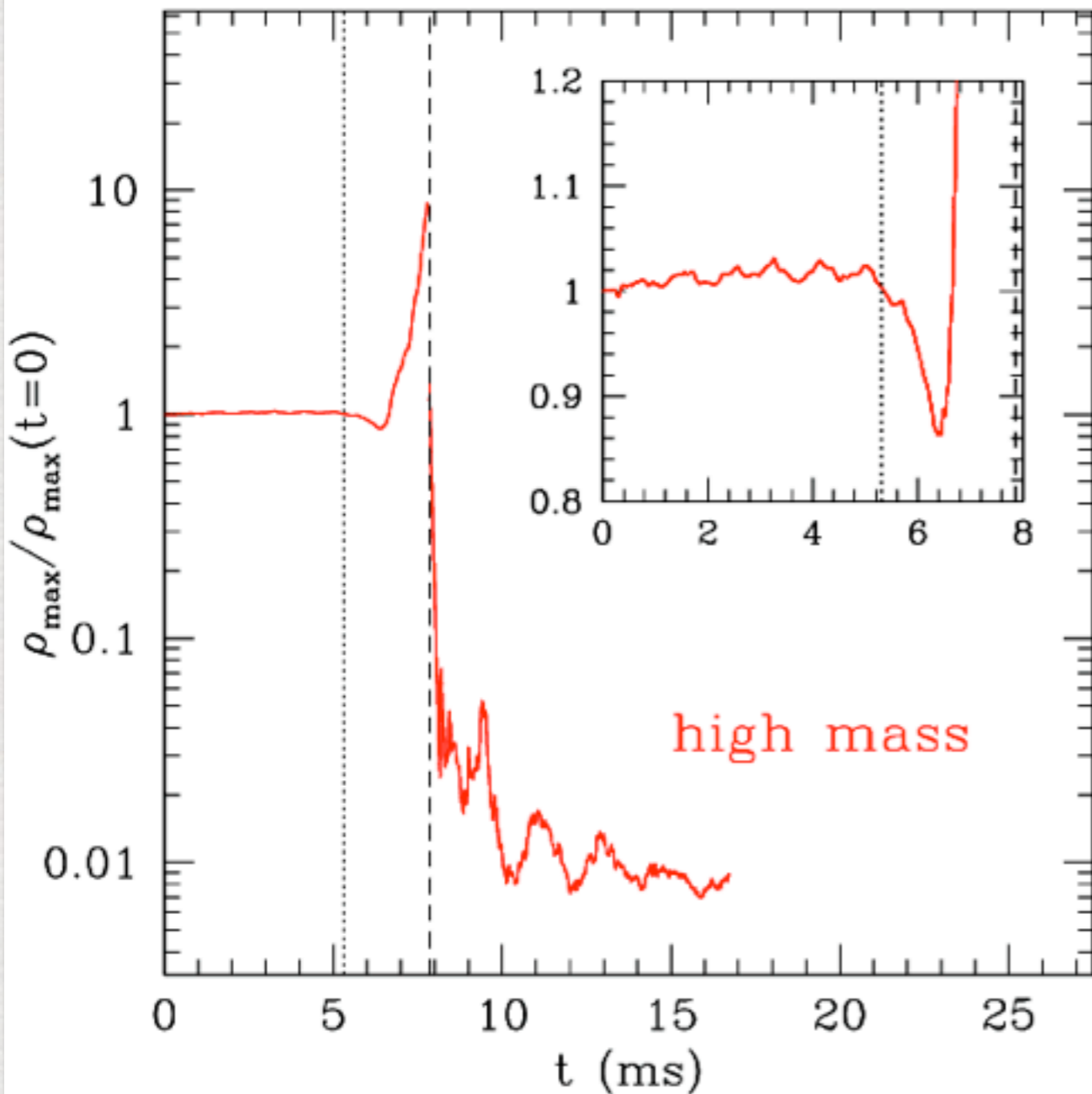


Density [ $\text{g}/\text{cm}^3$ ]

# Matter dynamics

high-mass binary

low-mass binary



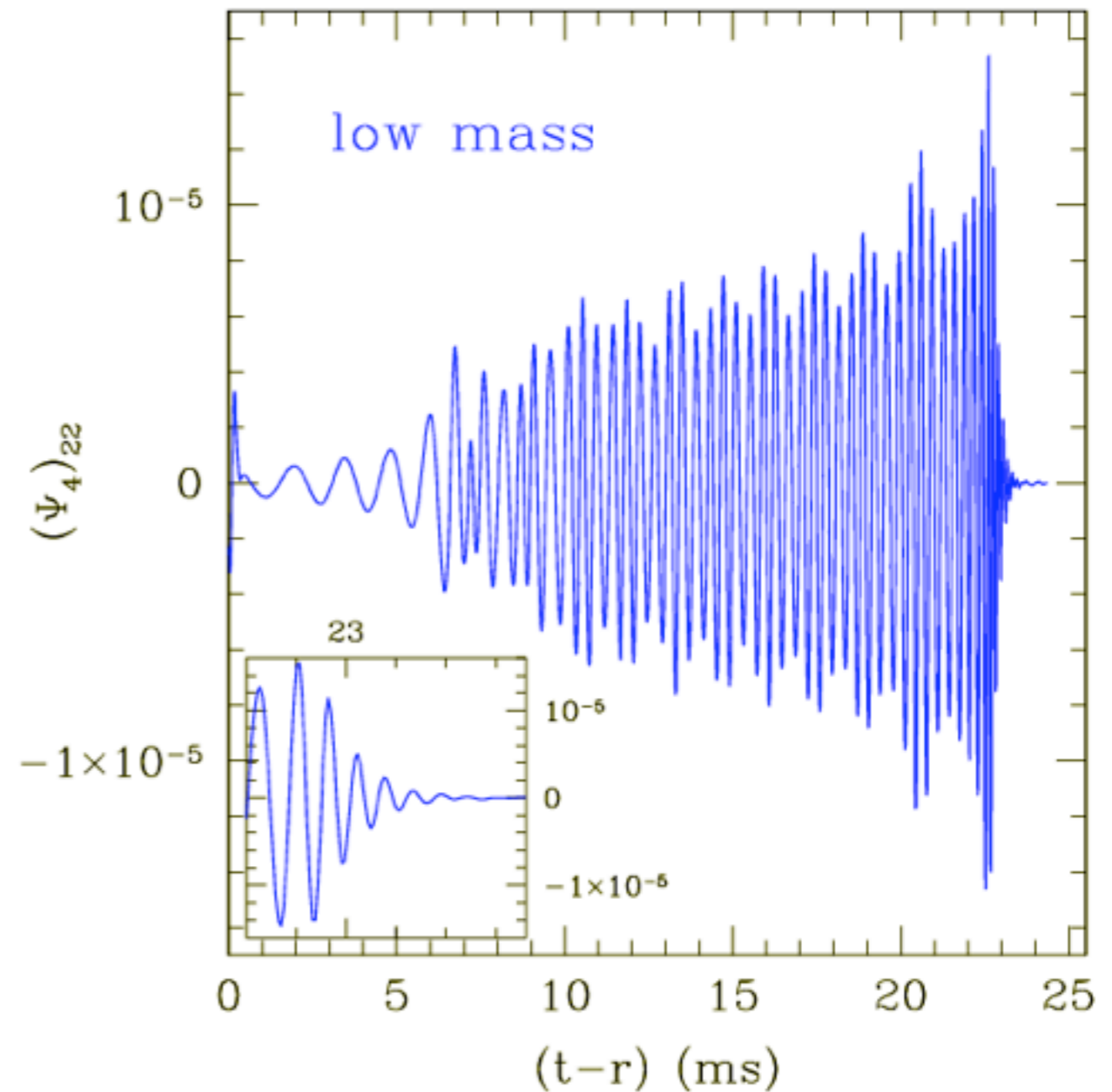
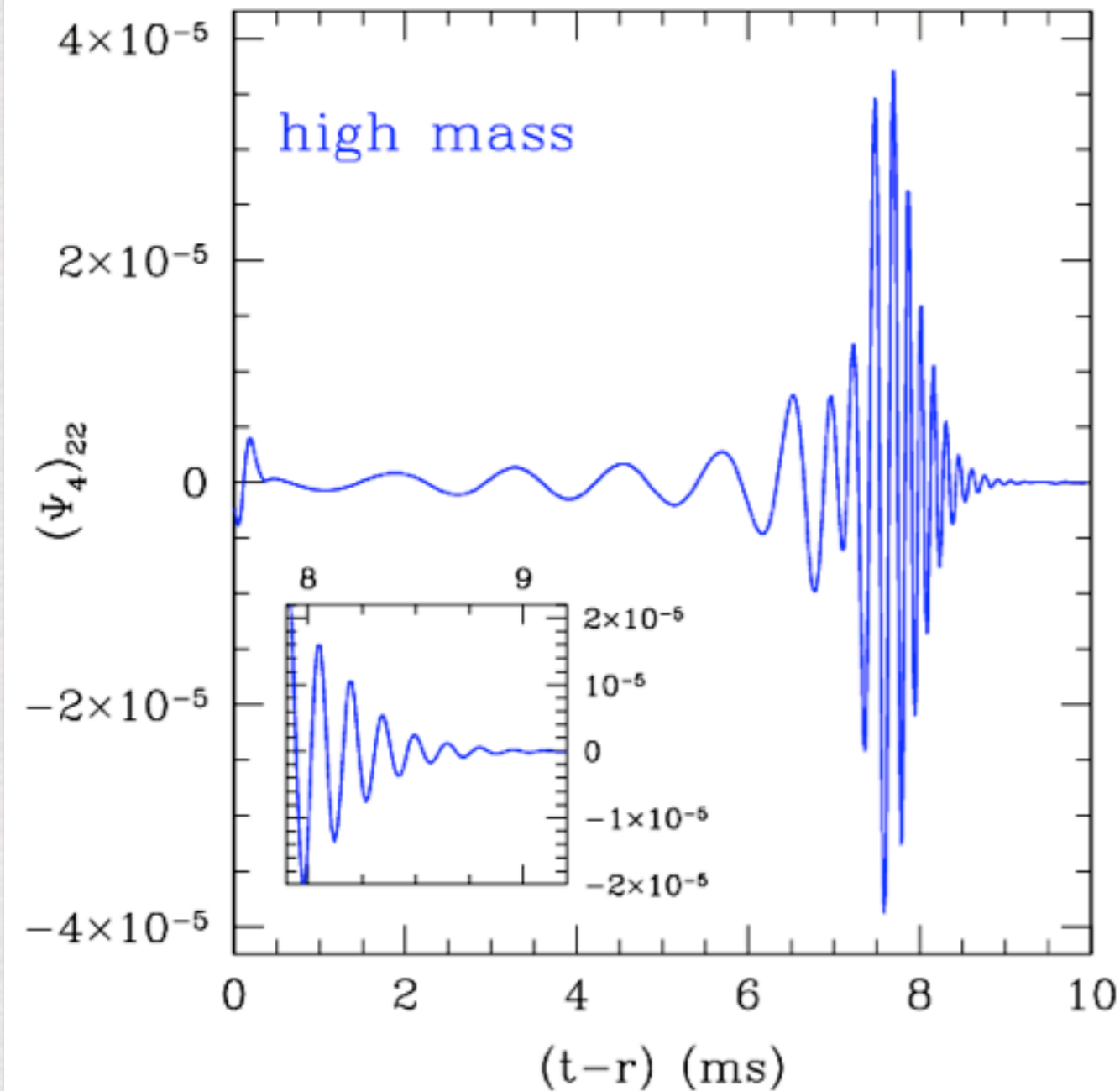
soon after the merge the torus is formed and undergoes oscillations

long after the merger a BH is formed surrounded by a torus

# Waveforms: polytropic EOS

high-mass binary

low-mass binary



first time the full signal from the formation to a bh has been computed

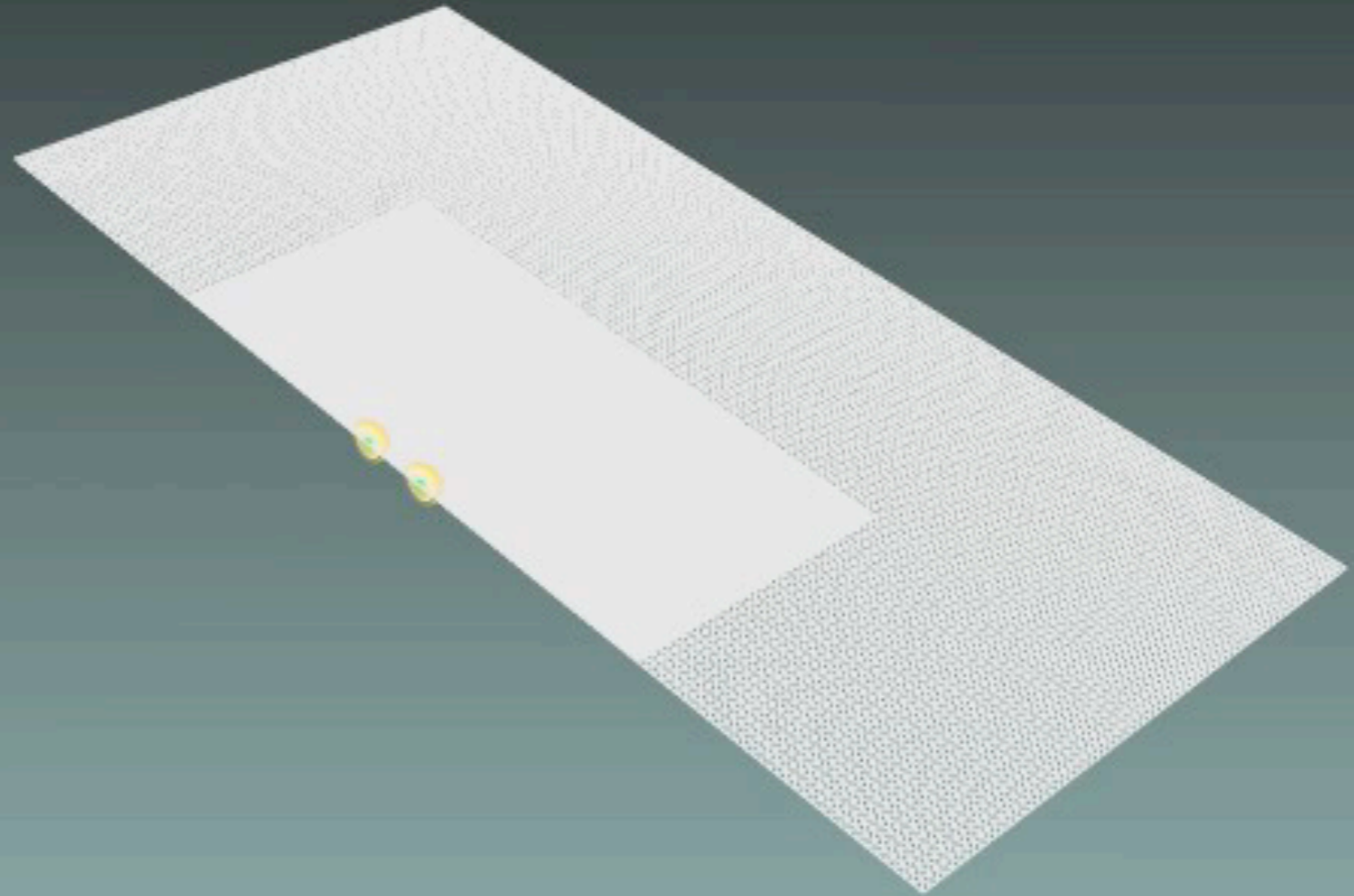
development of a bar-deformed NS leads to a long gw signal

Animations: Kaehler, Giacomazzo, Rezzolla

T[ms] = 0.00



T[M] = 0.00



Ideal-fluid EOS: high-mass binary

$$M = 1.6 M_{\odot}$$

0.0 6.1E+14

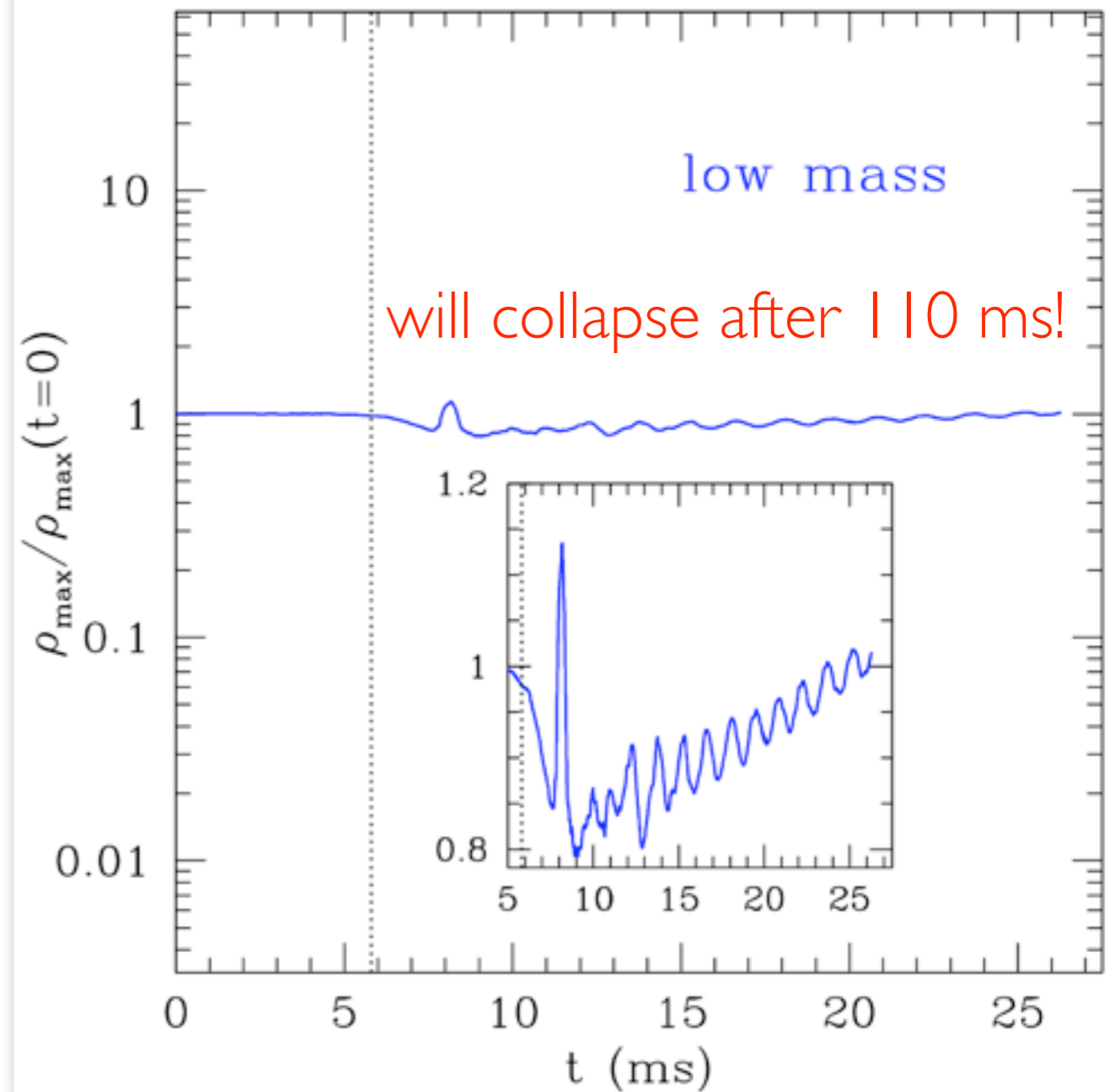
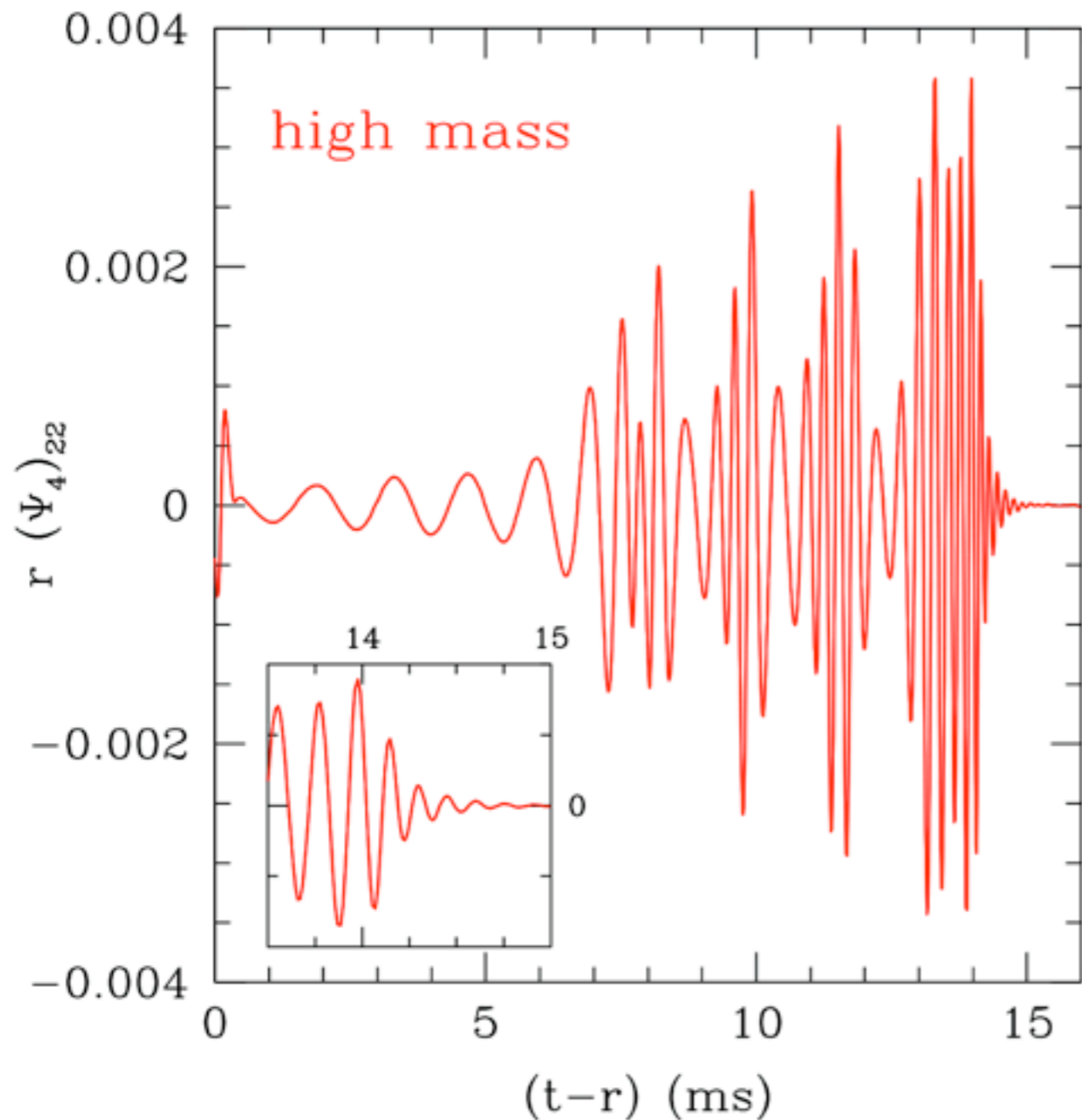


Density [g/cm<sup>3</sup>]

# Waveforms: ideal-fluid EOS

high-mass binary

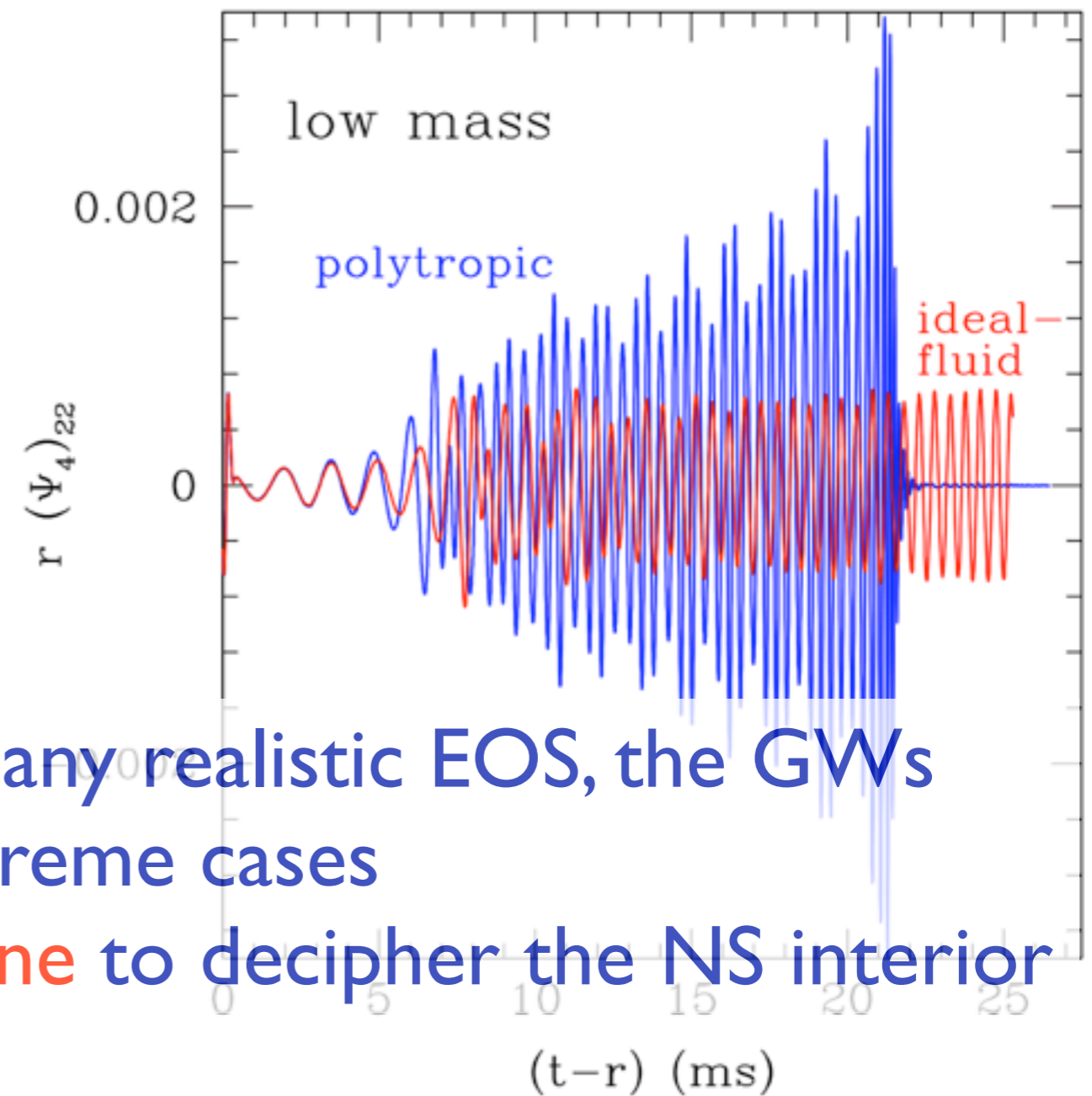
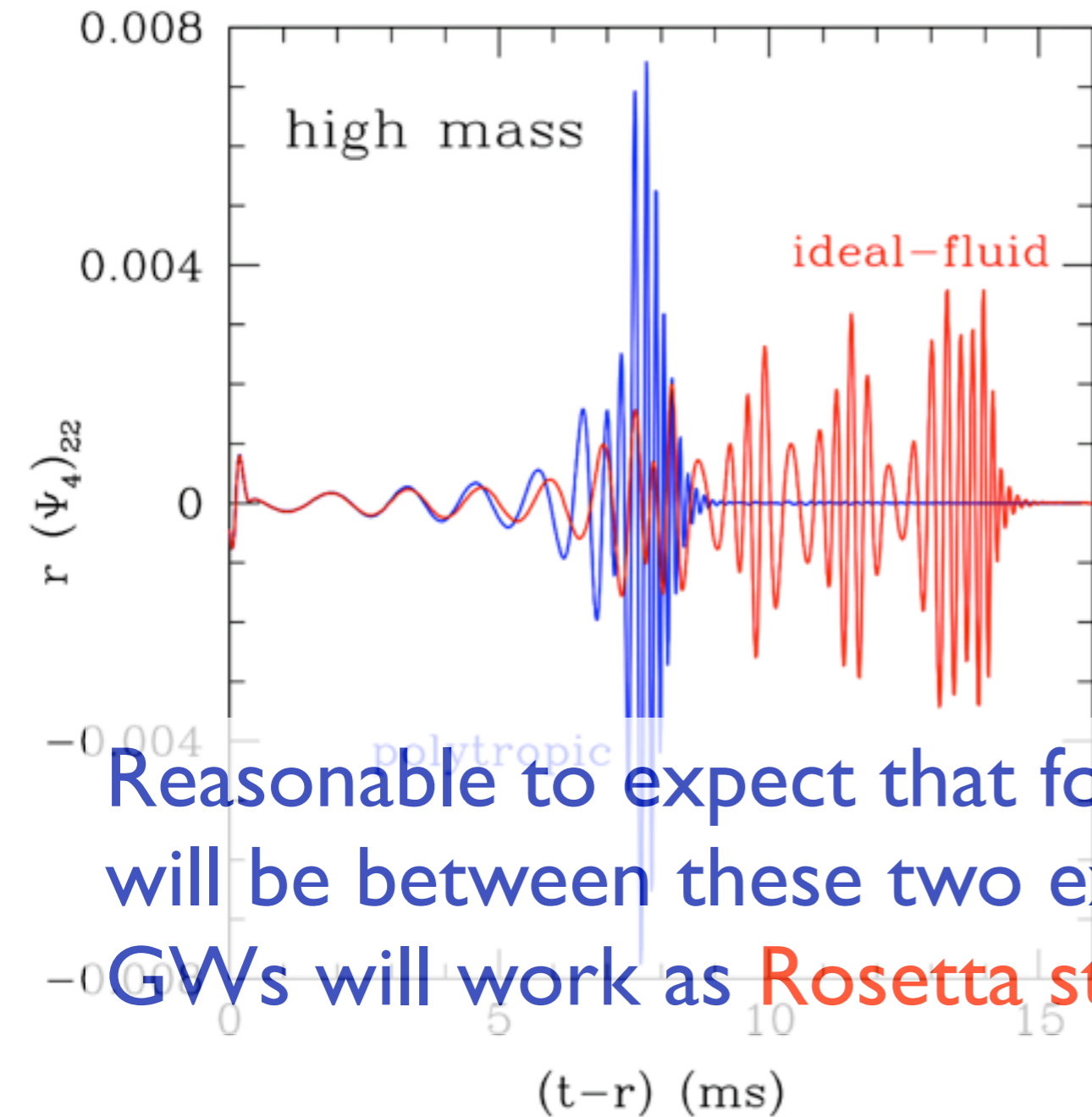
low-mass binary



the high internal energy (temperature) of the HMNS prevents a prompt collapse

the HMNS evolves on longer (radiation-reaction) timescale

# Imprint of the EOS: Ideal-fluid vs polytropic



Reasonable to expect that for any realistic EOS, the GWs will be between these two extreme cases

GWs will work as **Rosetta stone** to decipher the NS interior

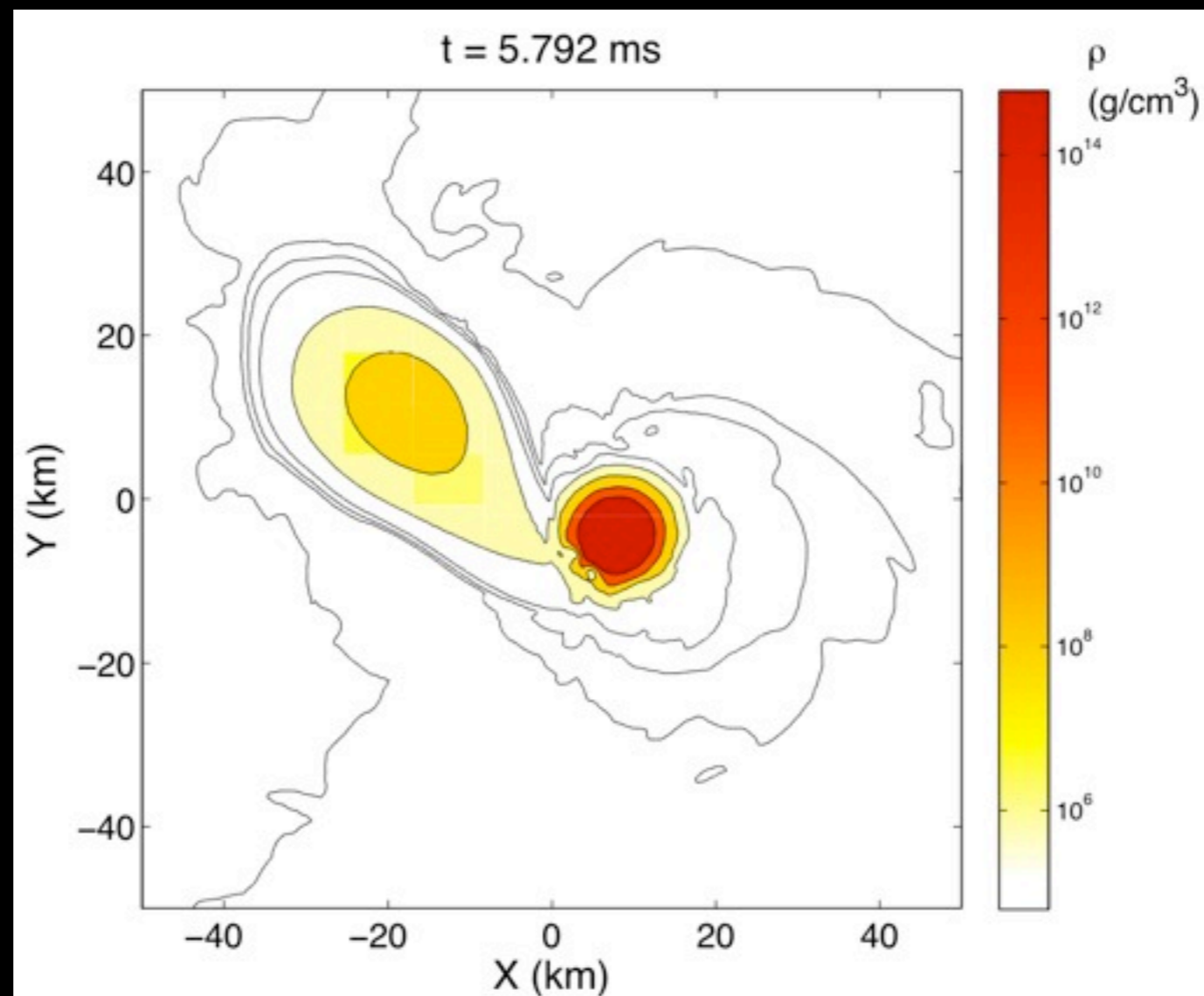
After the merger a BH is produced over a timescale **comparable** with the **dynamical** one

After the merger a BH is produced over a timescale **larger** or **much larger** than the **dynamical** one



# Unmagnetized **unequal**-mass binaries

Link, Rezzolla, Baiotti, Giacomazzo, to be submitted, 2009

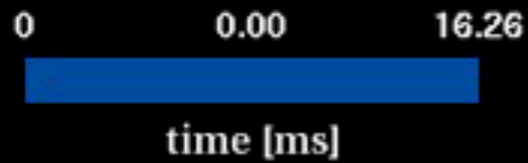


# Torus properties: unequal-masses

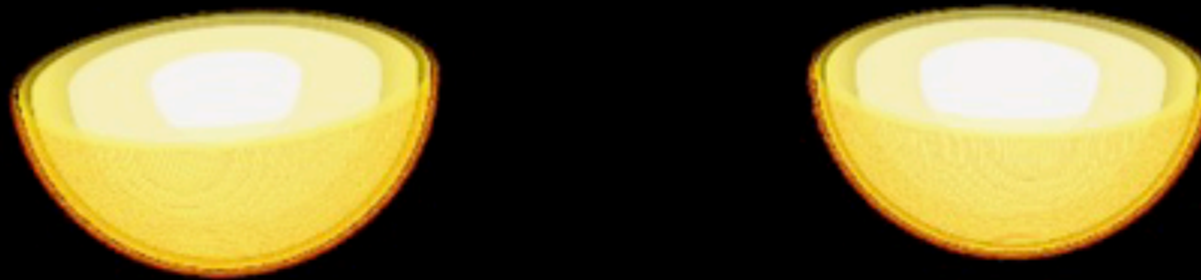
We have considered the inspiral and merger of 7 irrotational binaries with variable total mass and mass ratio (see table)

Model	$M_{\text{total}}$ ( $M_{\odot}$ )	$q$	$J$ ( $\text{g cm}^2/\text{s}$ )	$\nu_{\text{orbit}}$ (Hz)	$\rho_{\text{max}}$ ( $\text{g/cm}^3$ )	$M_{\text{torus}}$ ( $M_{\odot}$ )
M3.4q0.70	3.371	0.70	$7.98 \times 10^{49}$	298.47	$1.28 \times 10^{15}$	0.132
M3.4q0.80	3.375	0.80	$8.36 \times 10^{49}$	303.62	$9.21 \times 10^{14}$	0.120
M3.4q0.91	3.404	0.91	$8.33 \times 10^{49}$	299.06	$7.58 \times 10^{14}$	0.079
M3.5q0.75	3.464	0.75	$8.40 \times 10^{49}$	300.84	$1.27 \times 10^{15}$	0.097
M3.7q0.94	3.680	0.94	$9.37 \times 10^{49}$	306.56	$9.75 \times 10^{14}$	0.006
M3.6q1.00	3.558	1	$8.92 \times 10^{49}$	303.32	$7.58 \times 10^{14}$	0.001
M3.8q1.00	3.802	1	$9.85 \times 10^{49}$	309.70	$9.74 \times 10^{14}$	0.001

A lot to say about the torus properties but a movie summarizes most of them



Total mass :  $3.7 M_{\odot}$ ; mass ratio : 0.94;

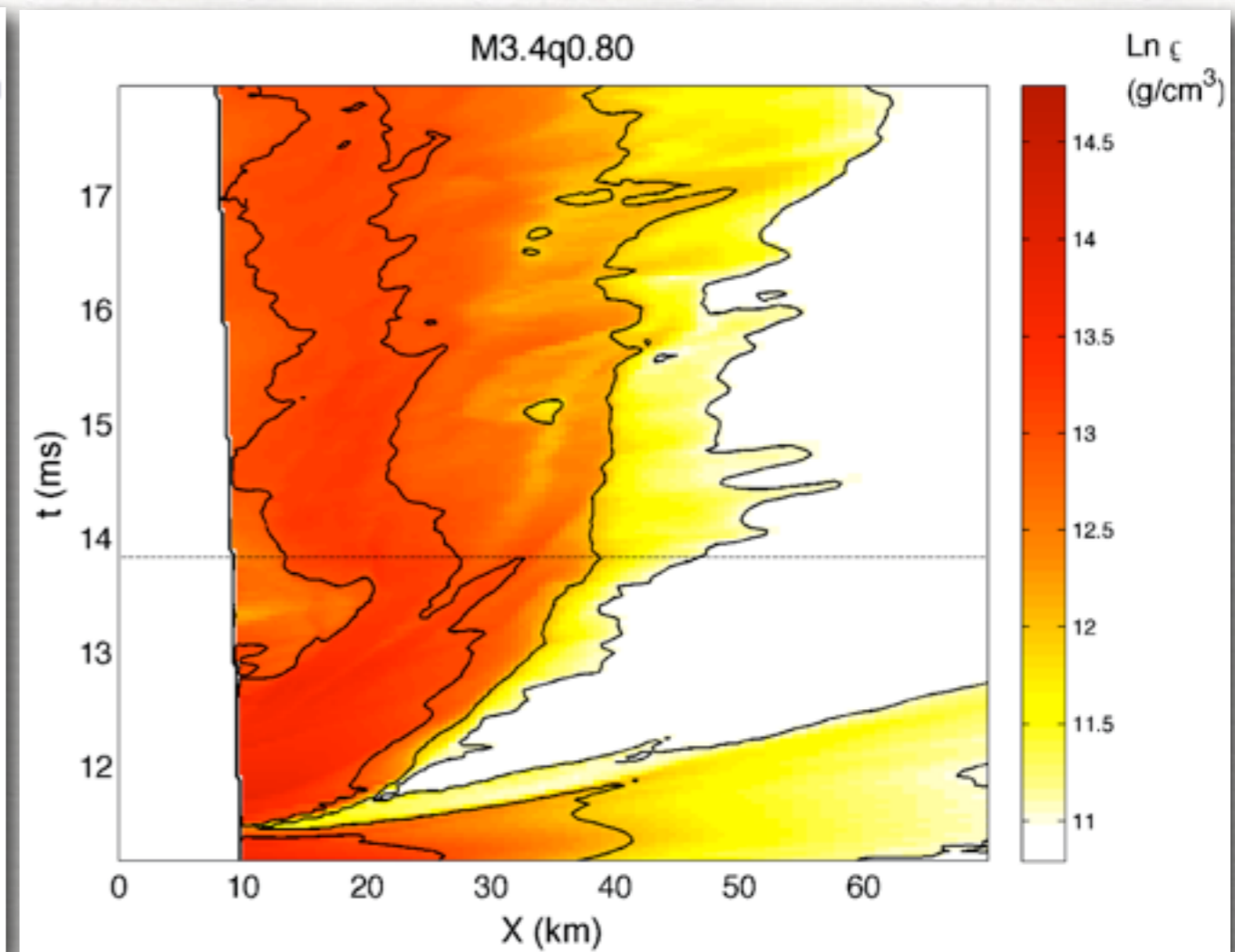
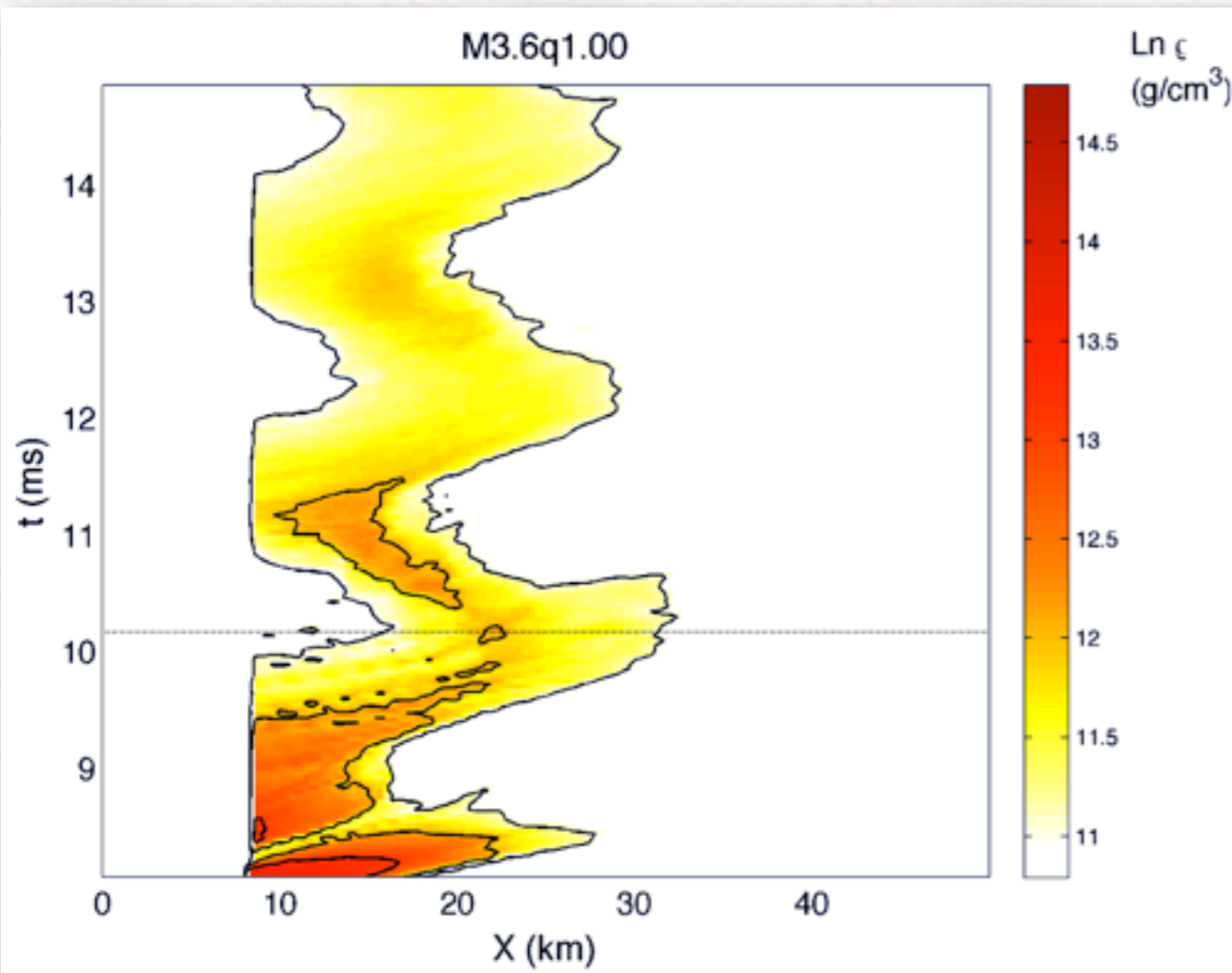


- \* the torii are generically more massive
- \* the torii are generically more extended
- \* the torii tend to a stable quasi-Keplerian configuration



# Torus properties: size

spacetime diagram of rest-mass density along x-direction

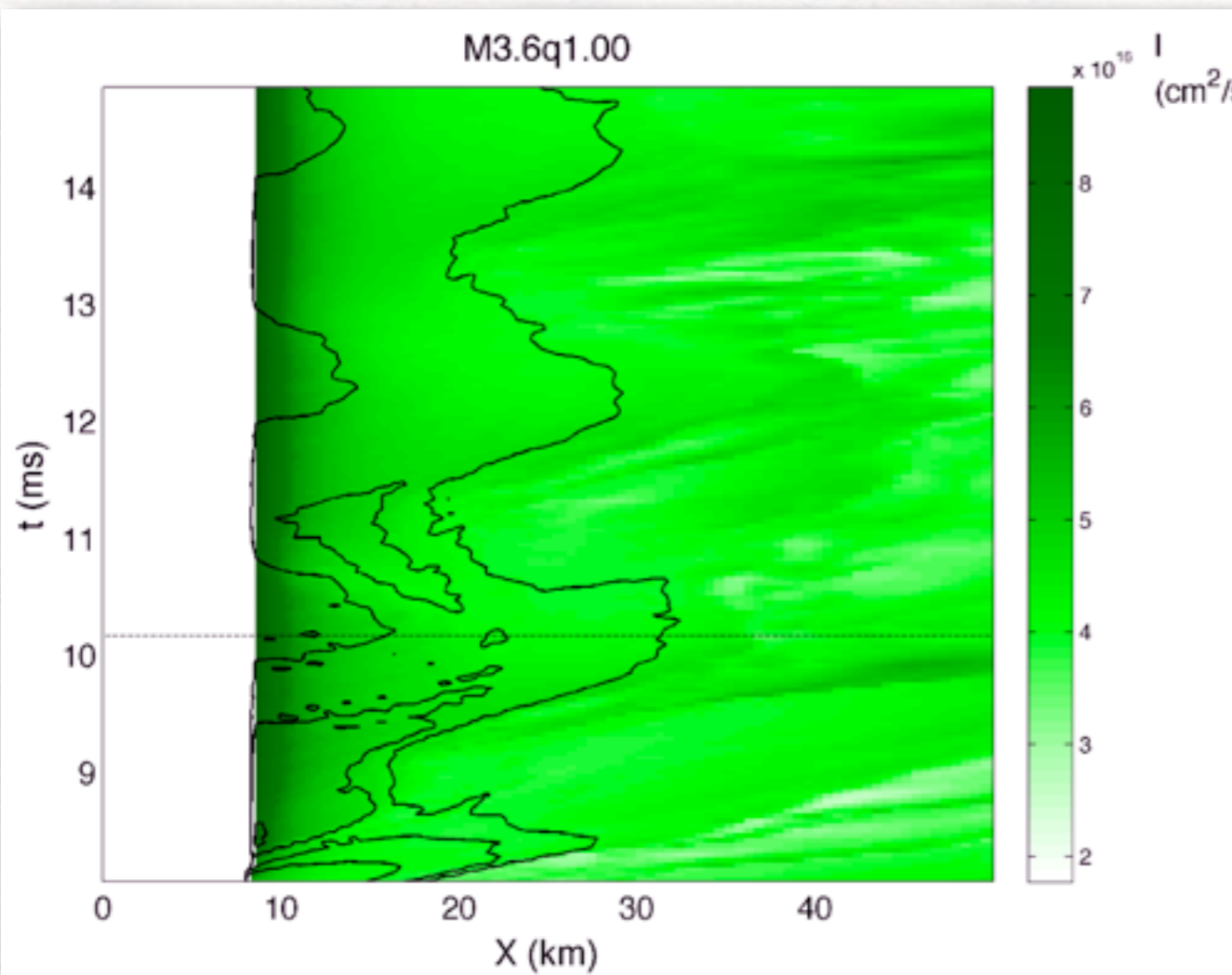


**equal** mass binary: note the **periodic** accretion and the **compact** size; densities are not very high

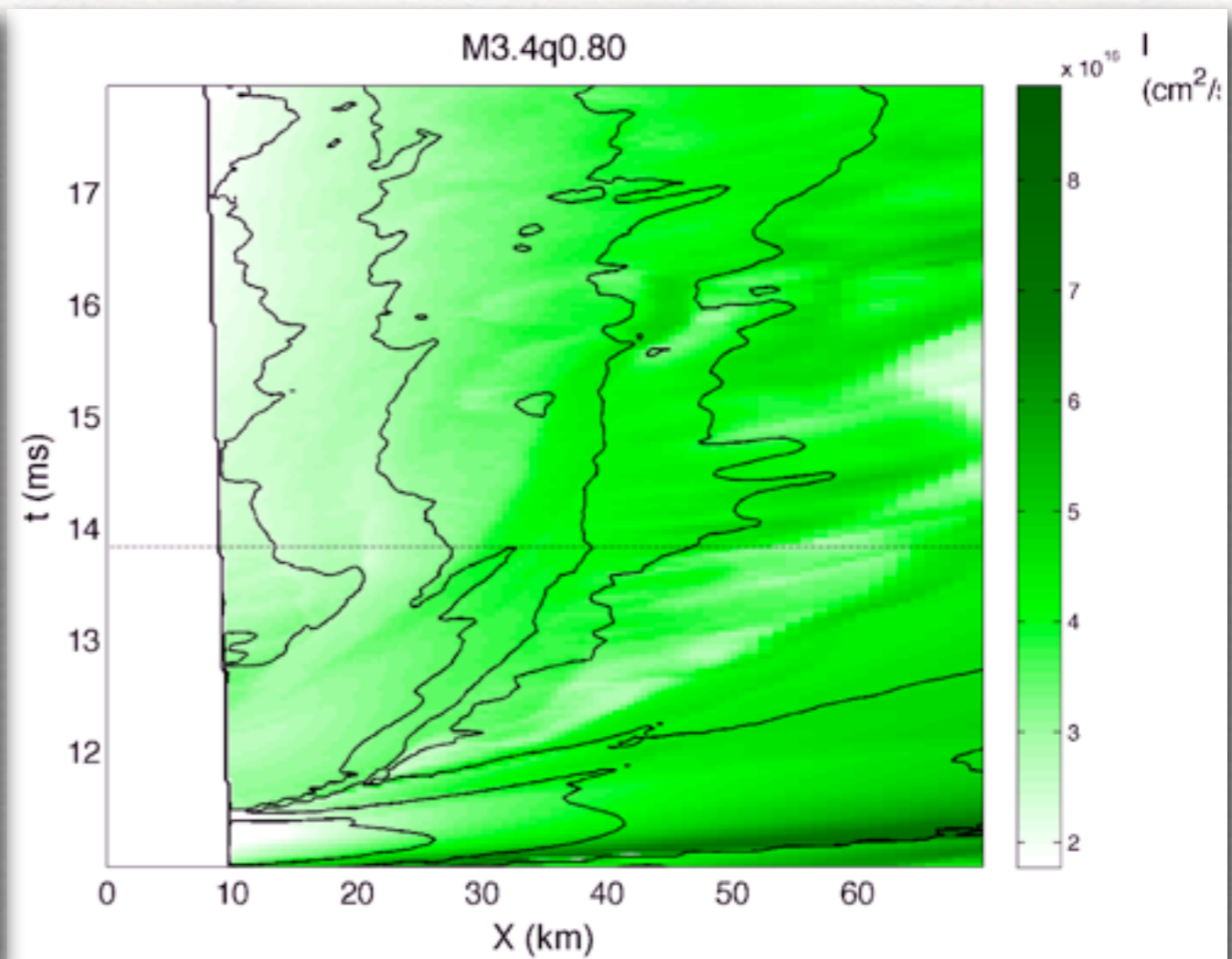
**unequal** mass binary: note the **continuous** accretion and the very **large** size and densities (temperatures)

# Torus properties: unequal-masses

spacetime diagram of specific angular mom.:  $\ell \equiv u_\phi / u_t$

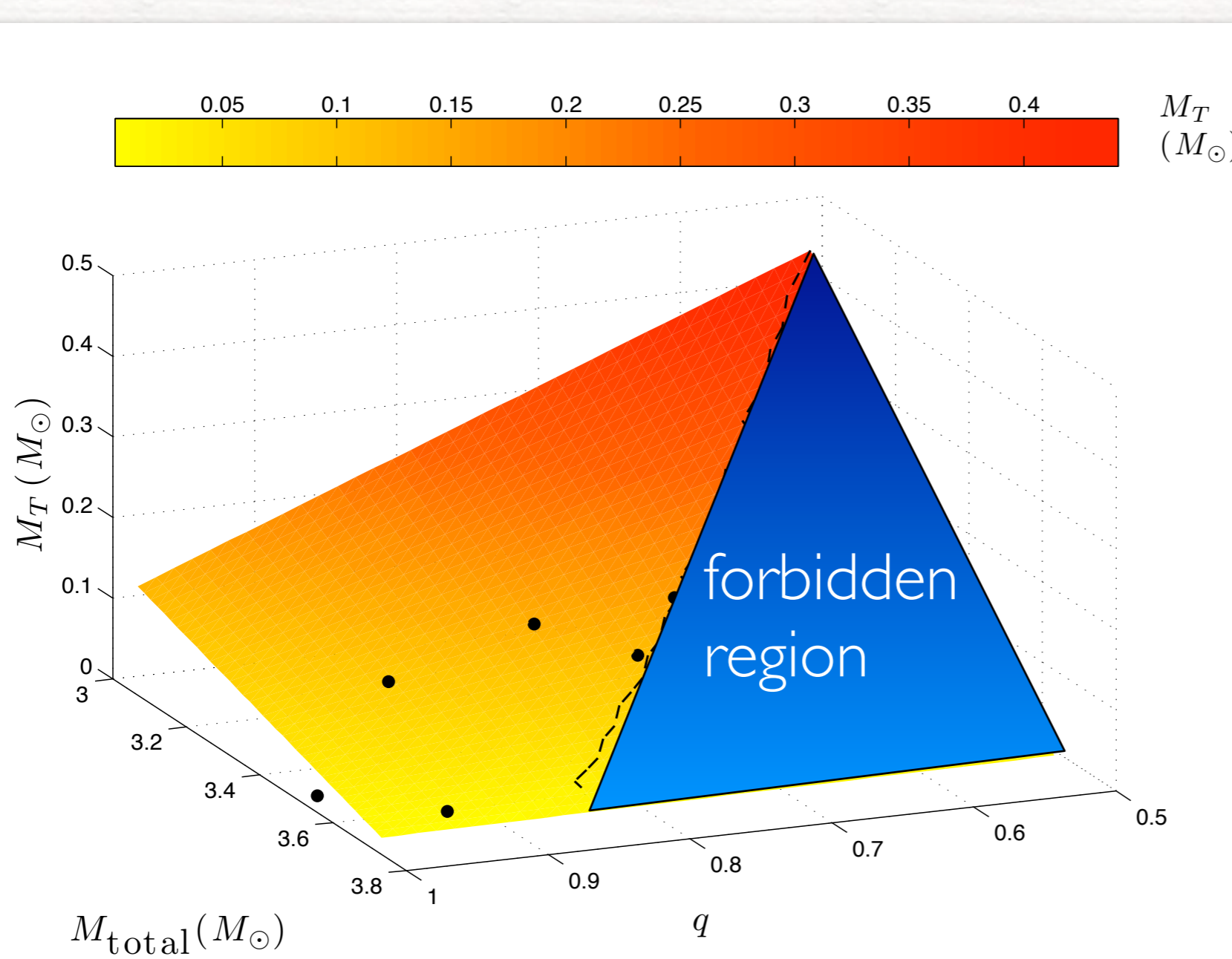


**equal** mass binary: specific angular momentum is larger at the inner edge and **decreases** outwards



**unequal** mass binary: specific angular momentum is smaller at inner edge and **increases** outwards

# Torus properties: unequal-masses



Model	$M_{\text{total}}$ ( $M_\odot$ )	$q$	$M_{\text{torus}}$ ( $M_\odot$ )
M3.4q0.70	3.371	0.70	0.132
M3.4q0.80	3.375	0.80	0.120
M3.4q0.91	3.404	0.91	0.079
M3.5q0.75	3.464	0.75	0.097
M3.7q0.94	3.680	0.94	0.006
M3.6q1.00	3.558	1	0.001
M3.8q1.00	3.802	1	0.001

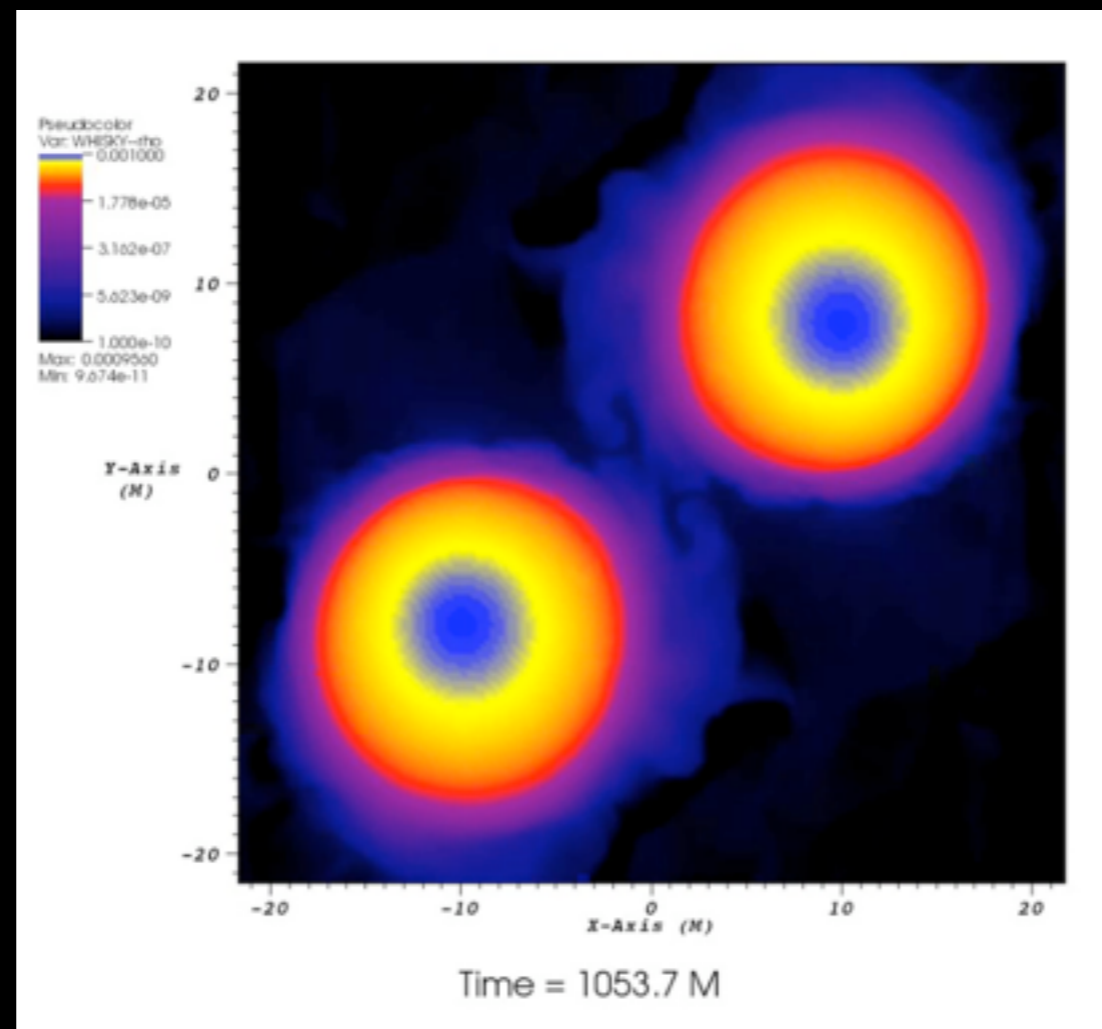
The torus mass decreases with the mass ratio and with the total mass; at lowest order:

$$M_{\text{torus}}(q, M_{\text{tot}}) = (1.16 - q)(M_{\text{max}} - M_{\text{tot}})$$

where  $M_{\text{max}}$  is the maximum (baryonic) mass of the binary

# Unmagnetized **unequal**-mass binaries

Giacomazzo, Rezzolla, Baiotti, MNRAS Lett. 2009



# Extending the work to MHD

We have considered the same models also when an initially poloidal magnetic field of  $\sim 10^{12}$  or  $\sim 10^{17}$  G is introduced

The magnetic field is added by hand using the vector potential:

$$A_{\phi} = A_b r^2 [\max(P - P_{cut}, 0)]^n$$

where  $A_b$  and  $P_{cut} = 0.04 \times \max(P)$  are two constants defining respectively the strength and the extension of the magnetic field inside the star.  $n=2$  defines the profile of the initial magnetic field.

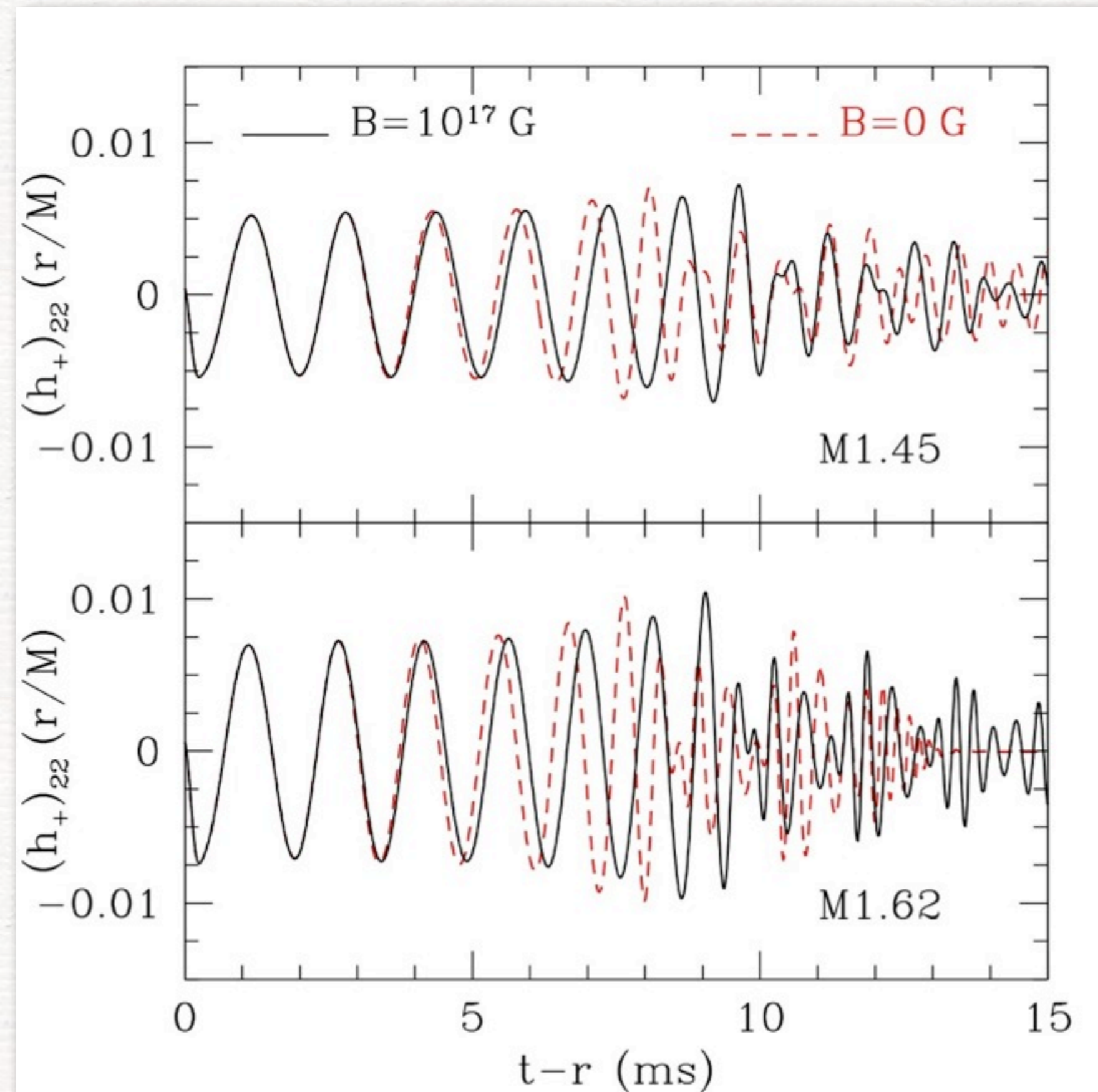
The initial magnetic fields are therefore fully contained inside the stars: ie no magnetospheric effects.

Simulated 8 binaries (low/high mass) with MFs:

$$B=0, 10^{12}, 10^{14}, 10^{17} \text{ G}$$



# Waveforms: comparing against magnetic fields



Comparing against magnetic field strengths the differences are much more evident:

- the **post-merger** evolution is different for all masses (and essentially also for all MFs); strong MF delay the collapse to BH
- the evolution in the **inspiral** is also different for such large MFs

This confirms Anderson et al (2008). Is this true also for smaller MFs?

# Understanding the dependence on MF

To quantify the differences and determine whether detectors will see a difference in the inspiral, we calculate the **overlap**

$$\mathcal{O}[h_{B1}, h_{B2}] \equiv \frac{\langle h_{B1} | h_{B2} \rangle}{\sqrt{\langle h_{B1} | h_{B1} \rangle \langle h_{B2} | h_{B2} \rangle}}$$

where the scalar product is

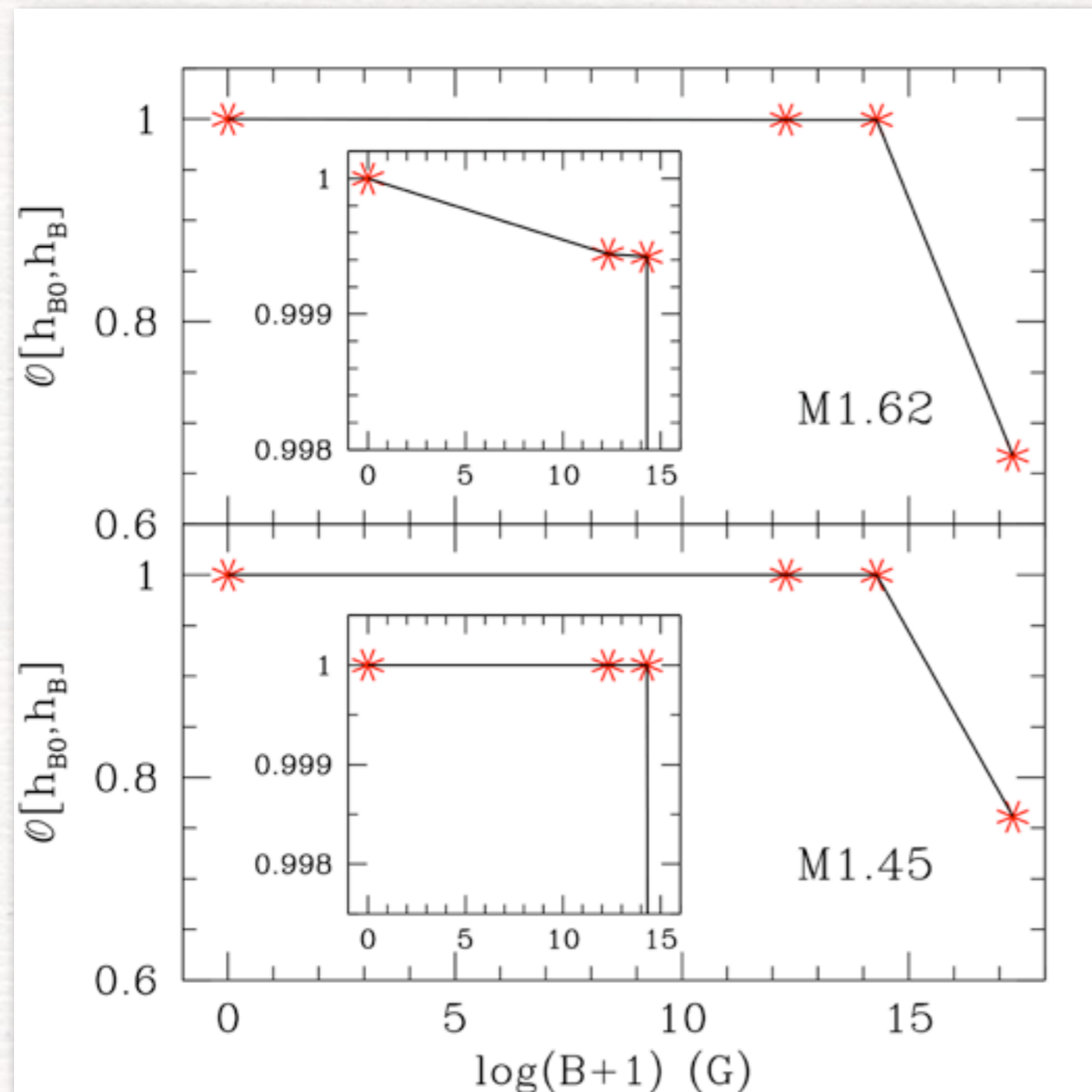
$$\langle h_{B1} | h_{B2} \rangle \equiv 4\Re \int_0^\infty df \frac{\tilde{h}_{B1}(f) \tilde{h}_{B2}^*(f)}{S_h(f)}$$

In essence, at these res:

$$\mathcal{O}[h_{B0}, h_B] \gtrsim 0.999$$

for  $B \lesssim 10^{17}$  G

Because the match is even higher for lower masses, **the influence of MFs on the inspiral is unlikely to be detected!**



# Nonlinear hydrodynamics at work

Quite clearly, the two stars do not merge with a frontal (head-on) collision.

Rather, during the merger a shear interface forms across which the velocities are discontinuous.

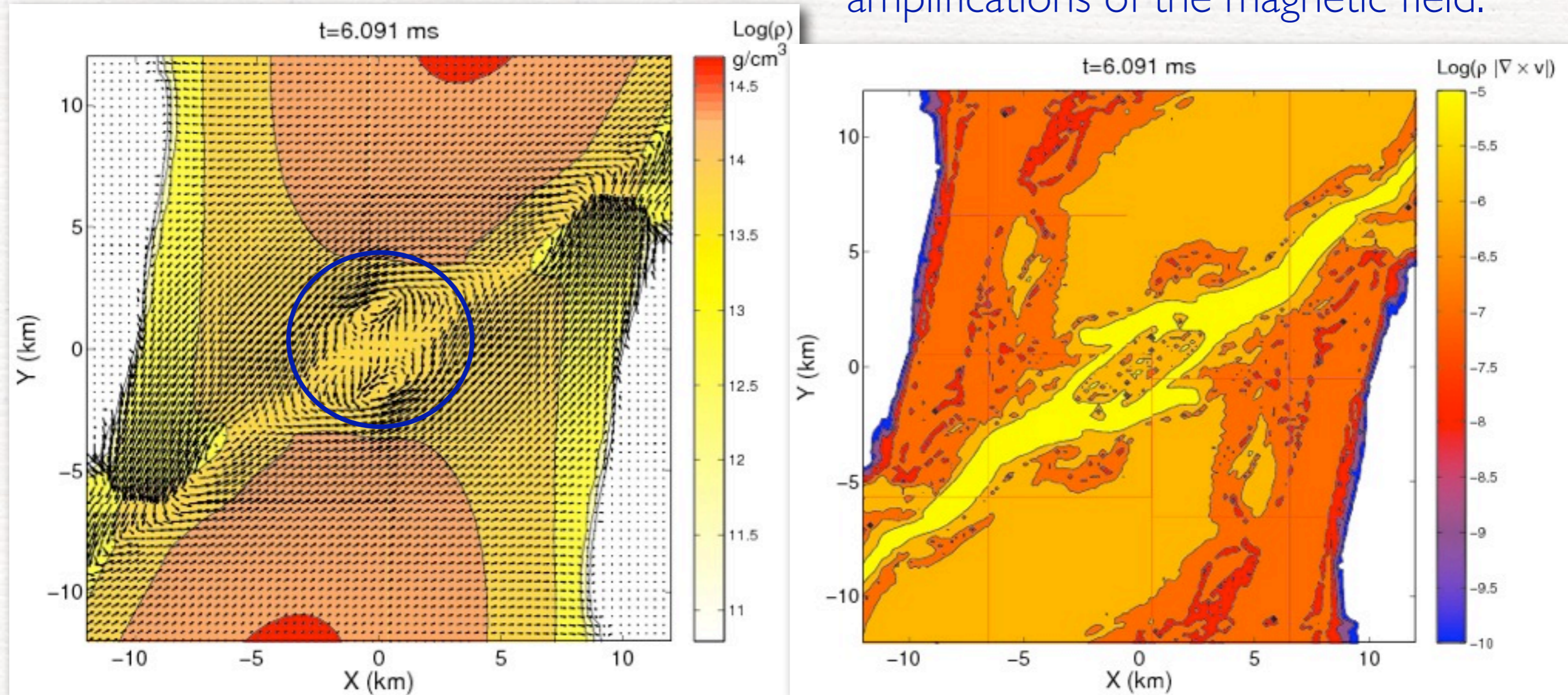
This leads to the formation of **vortices** and of a **Kelvin-Helmoltz** instability and a possible turbulent motion.

The instability can be quite important if the stars are magnetized

# KH instability in the high-mass binary

Note the development of vortices in the shear boundary layer produced at the time of the merger

More evident in terms of the weighted vorticity. In these regions one expects (and sees) large amplifications of the magnetic field.

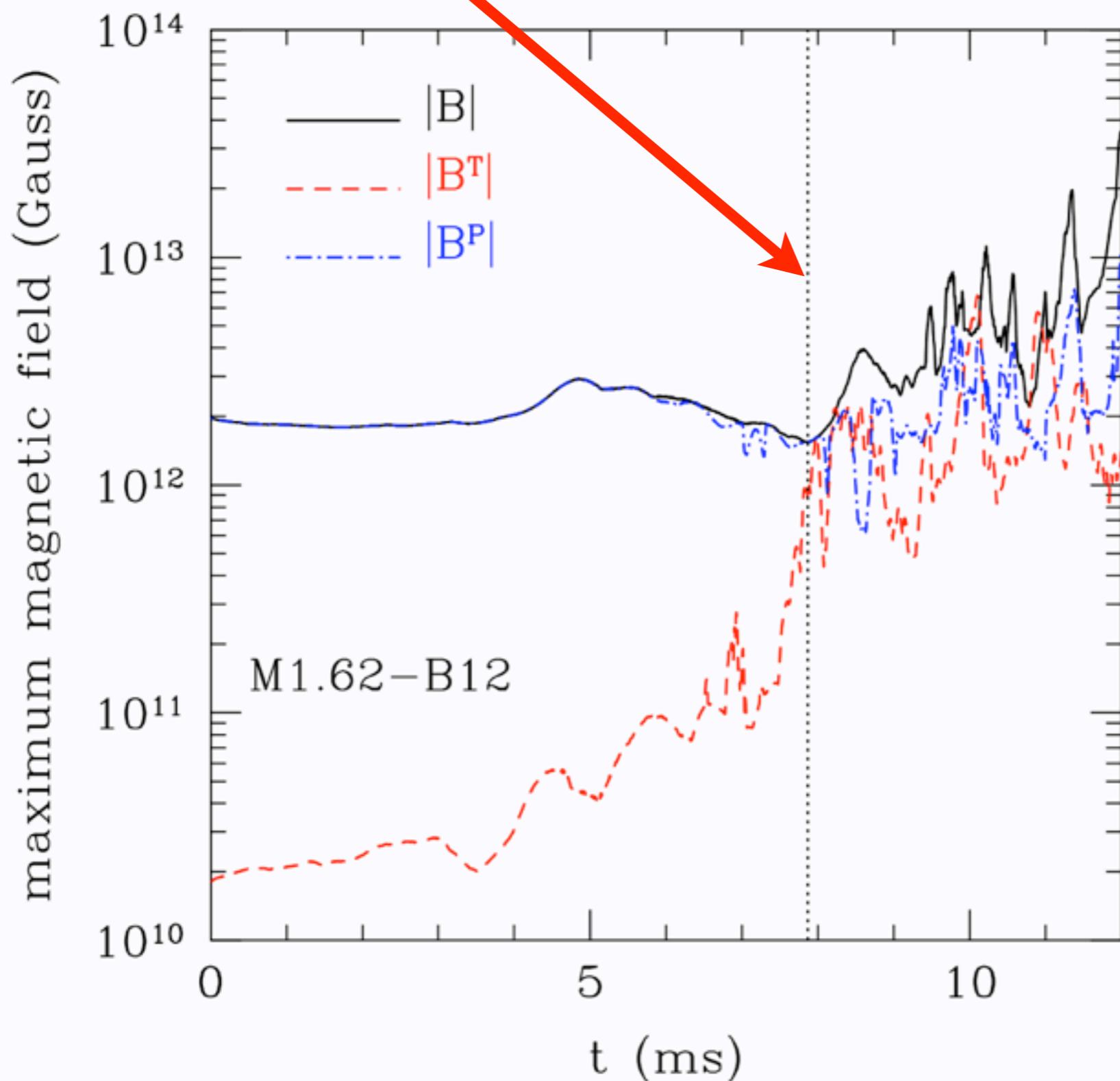


$(v^x, v^y)$  in "corotating" frame

$$\rho |\nabla \times v|^z$$

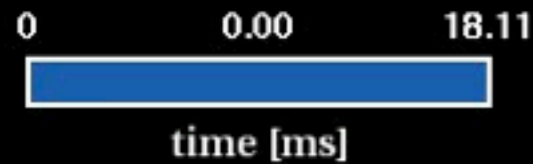
# Magnetic field evolution

Merger

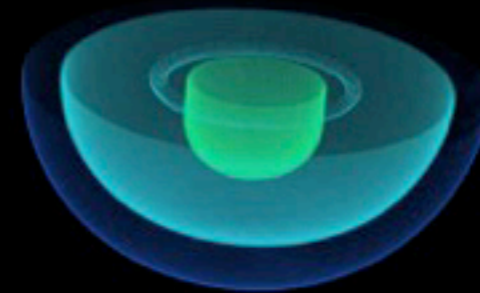
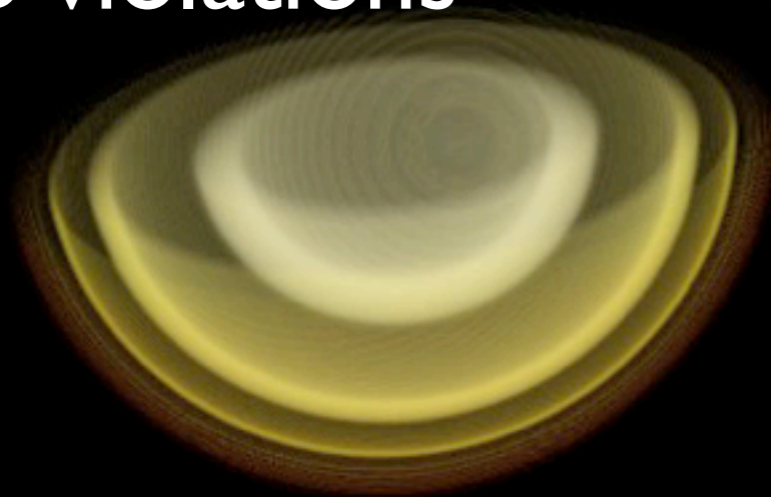


After merger the MF is amplified of one order of magnitude. The newly produced MF field is mostly toroidal and is clearly correlated with the increase in vorticity

First evidence in full GR that a MF field can be increased exponentially by the KH instability (Price & Rosswog, 2006)

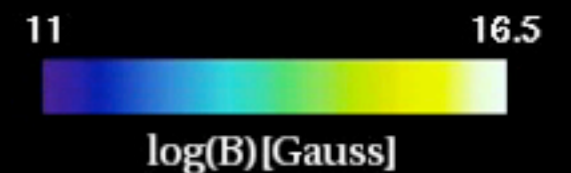


Note that the torus is much less dense and a large plasma outflow is starting to be launched. The evolution has been stopped because of excessive div-B violations

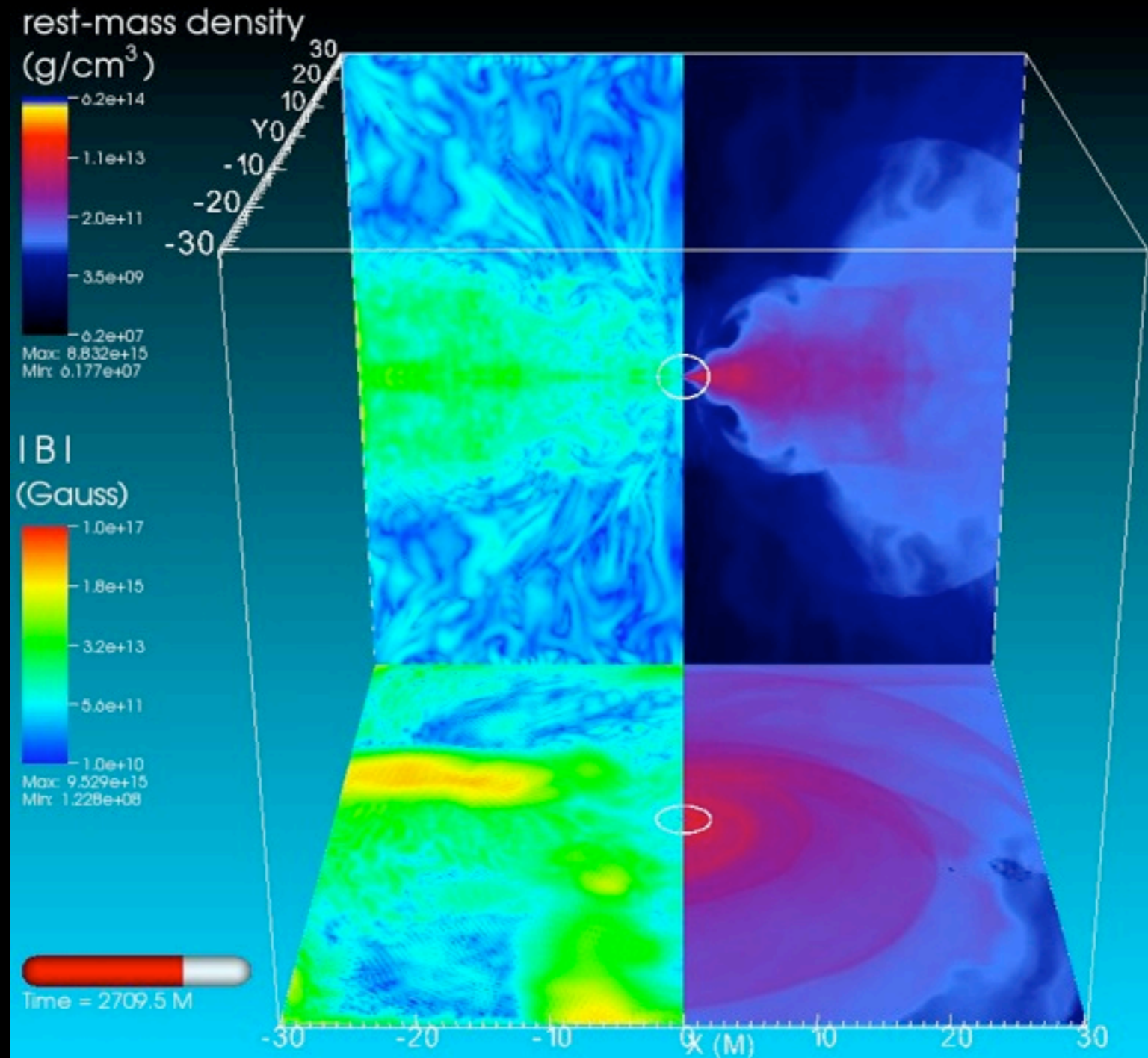


Typical evolution for a magnetized binary

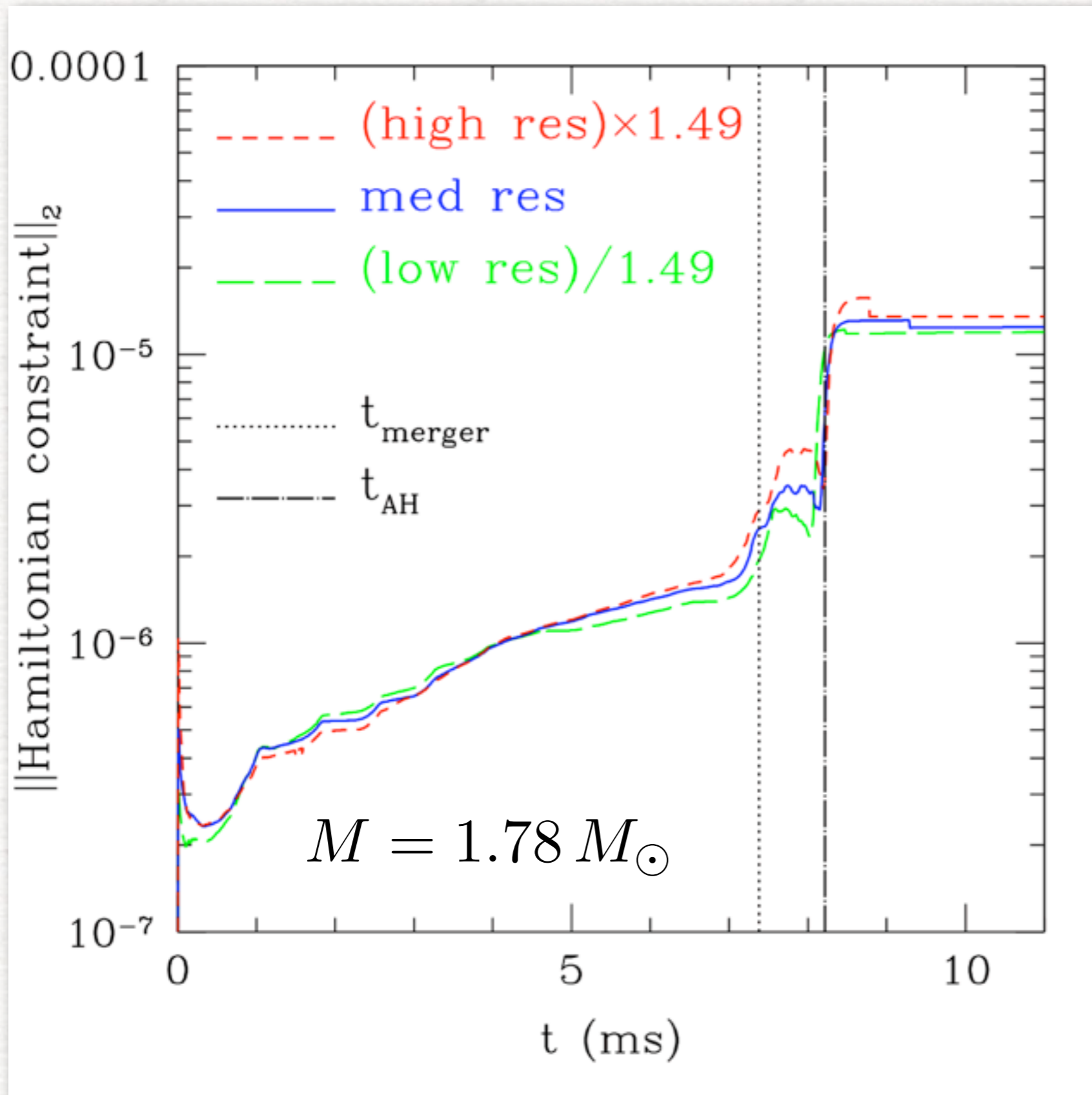
Ideal – fluid,  $M = 1.65 M_{\odot}$ ,  $B = 10^{12}$  G



# Difficulties requiring extra care!



# Postmerger complications

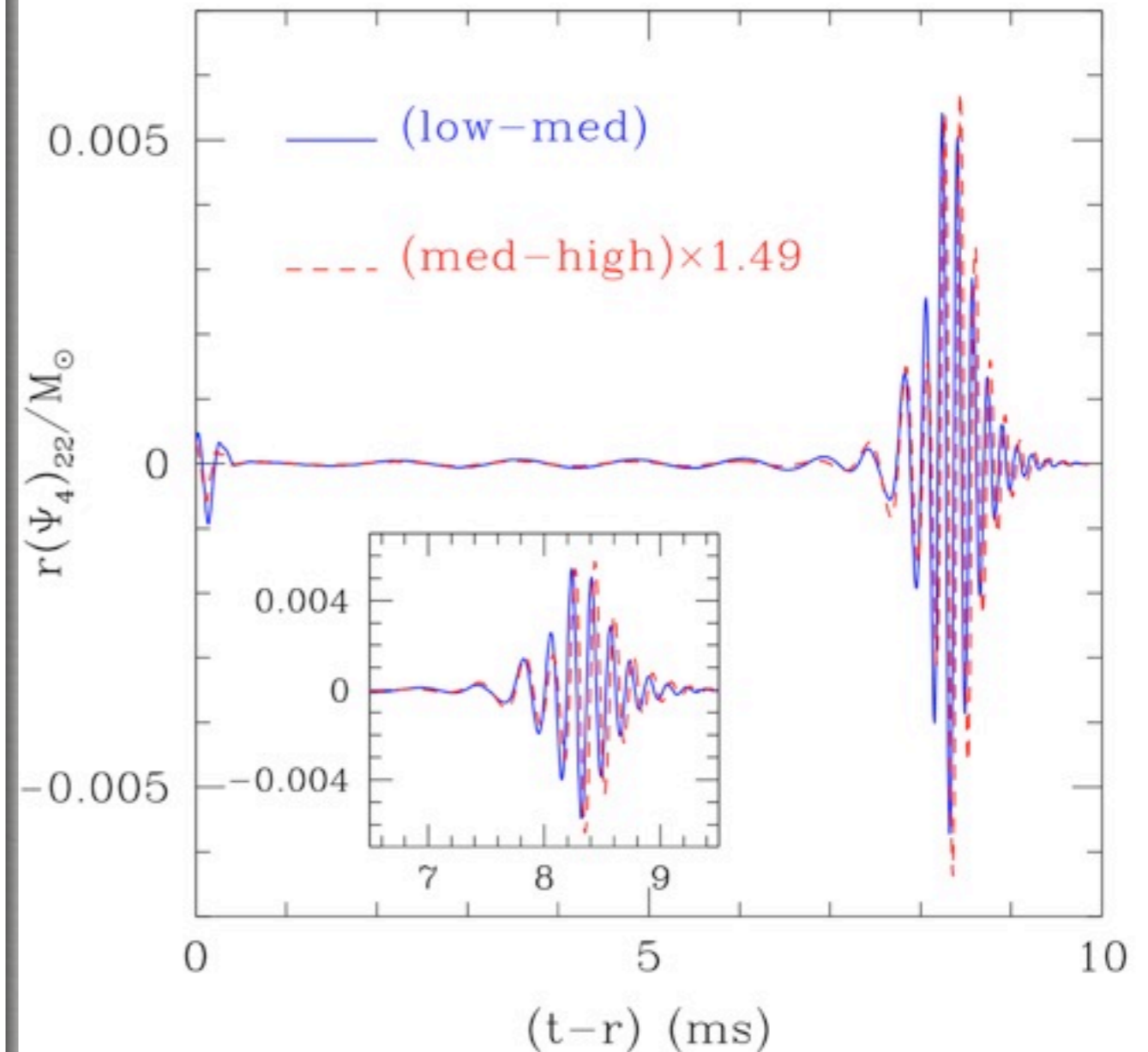
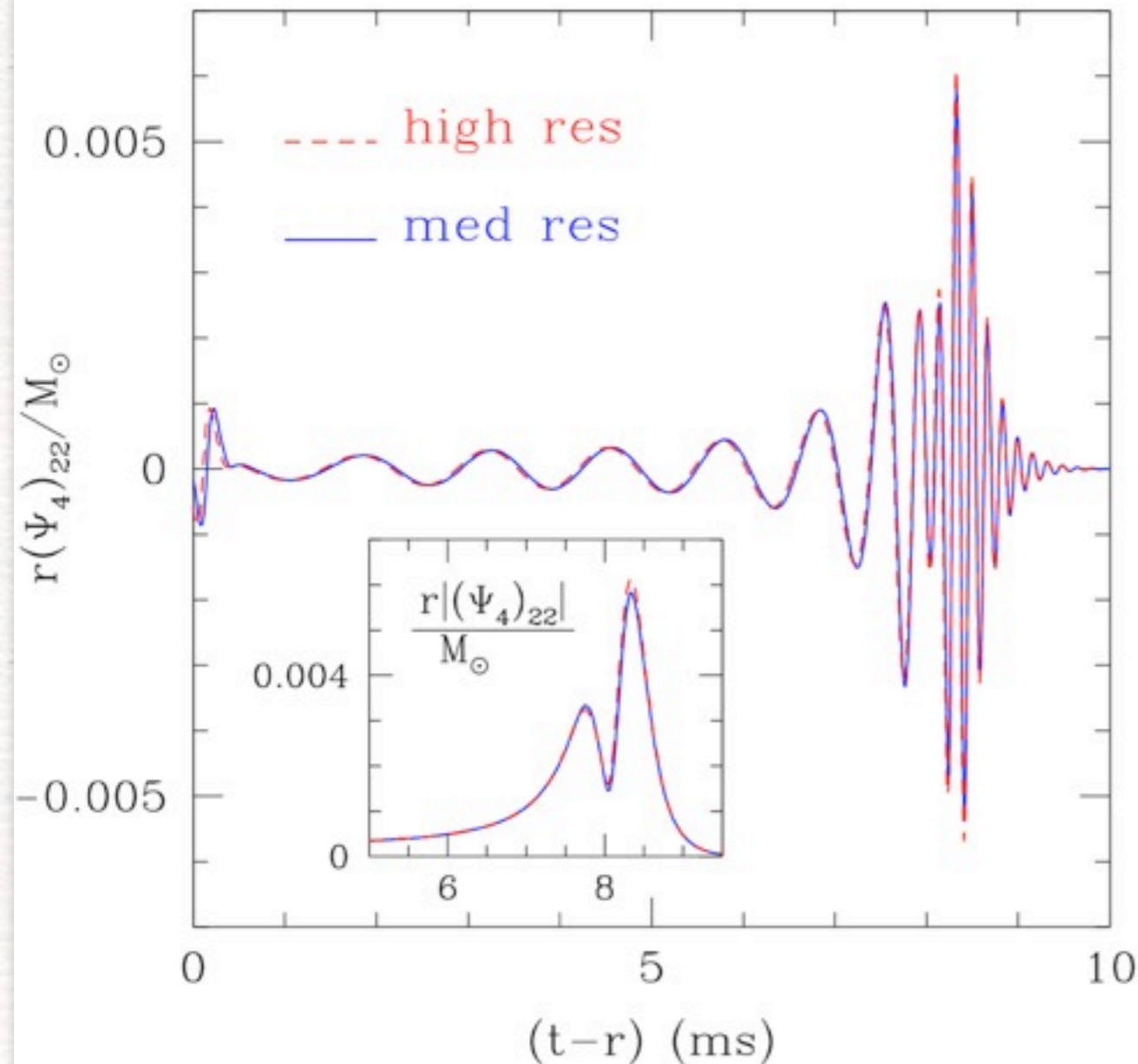


While high-order finite differencing is used for the Einstein eqs, the overall truncation error is the one of the matter eqs (true even for spectral solvers).

Even using high (3rd) order reconstruction, eg **PPM**, the overall convergence order is  $\sim 2$  during the inspiral. At the merger strong shocks reduce the convergence to  $\sim 1.2$ !



# Postmerger complications

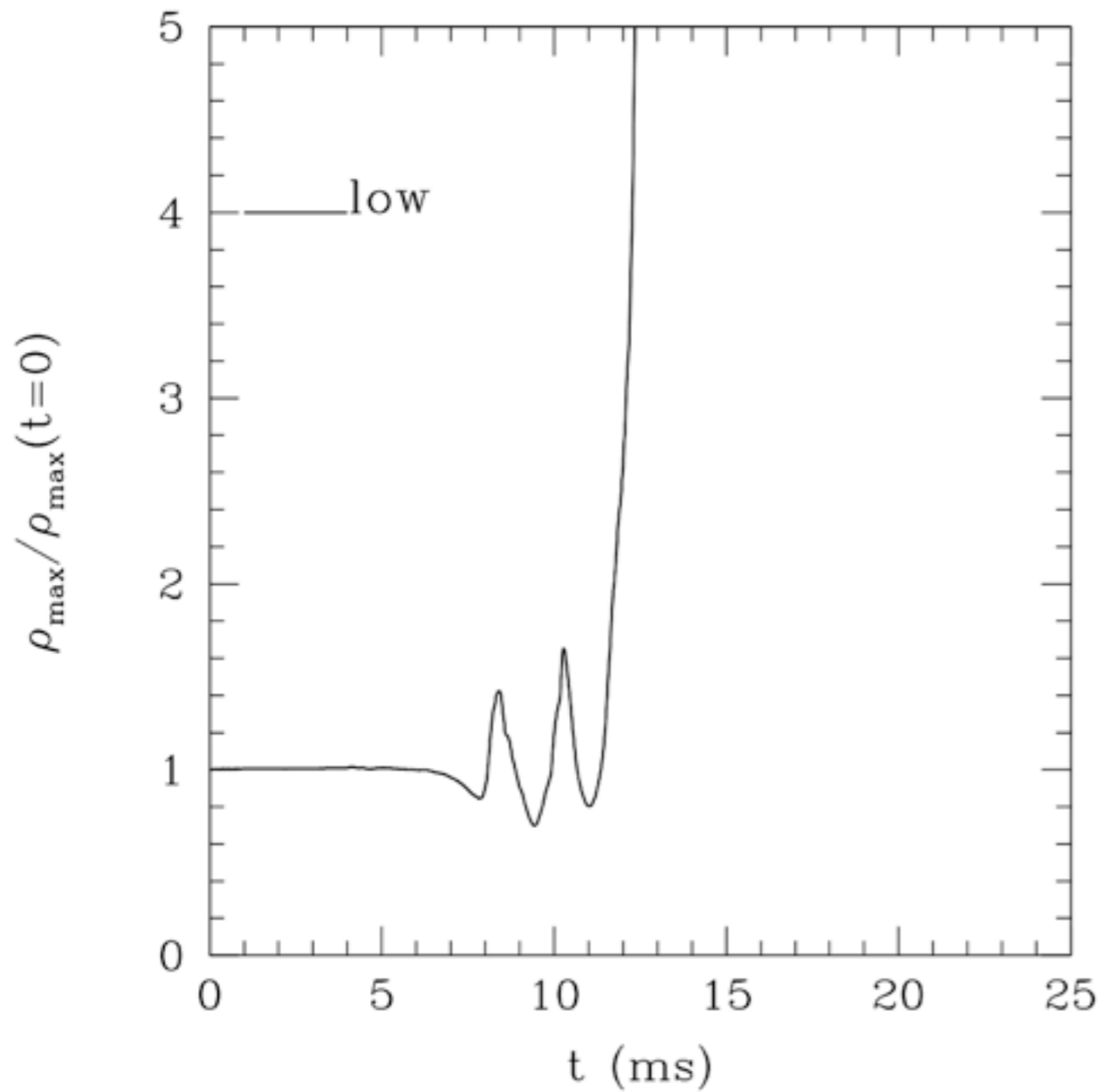


Waves at different resolutions; see Hannam & Hawke (0908.3139) on how to use them for the accuracy needed in 3d generation detectors.

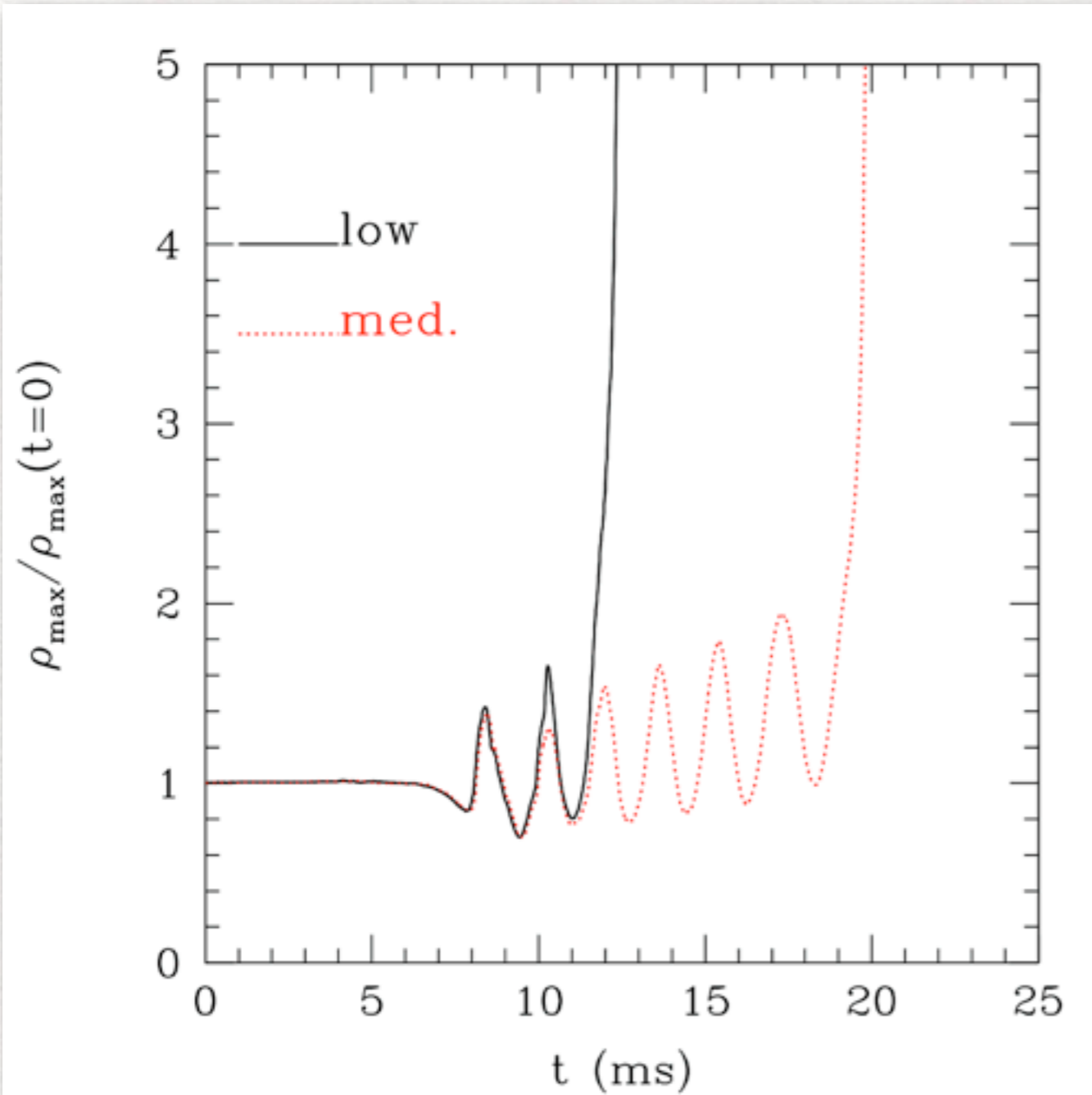
Indeed they are second order convergent: the coeff. of the  $O(h)$  is always smaller than  $O(h^2)$

# Postmerger nightmares..

High-mass:  $1.6 M_{\text{sun}}$ ,  
ideal-fluid EOS

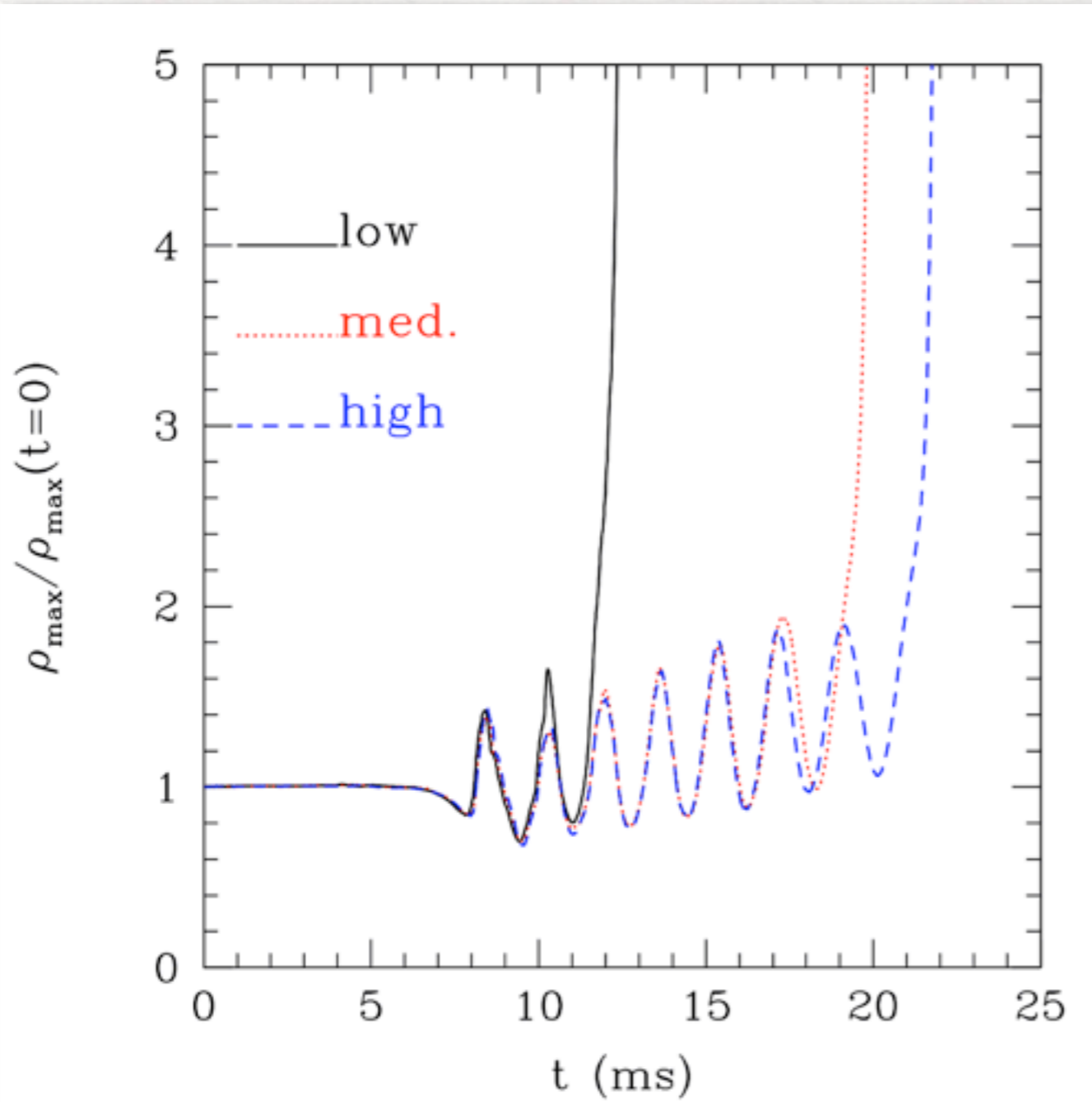


# Postmerger nightmares..



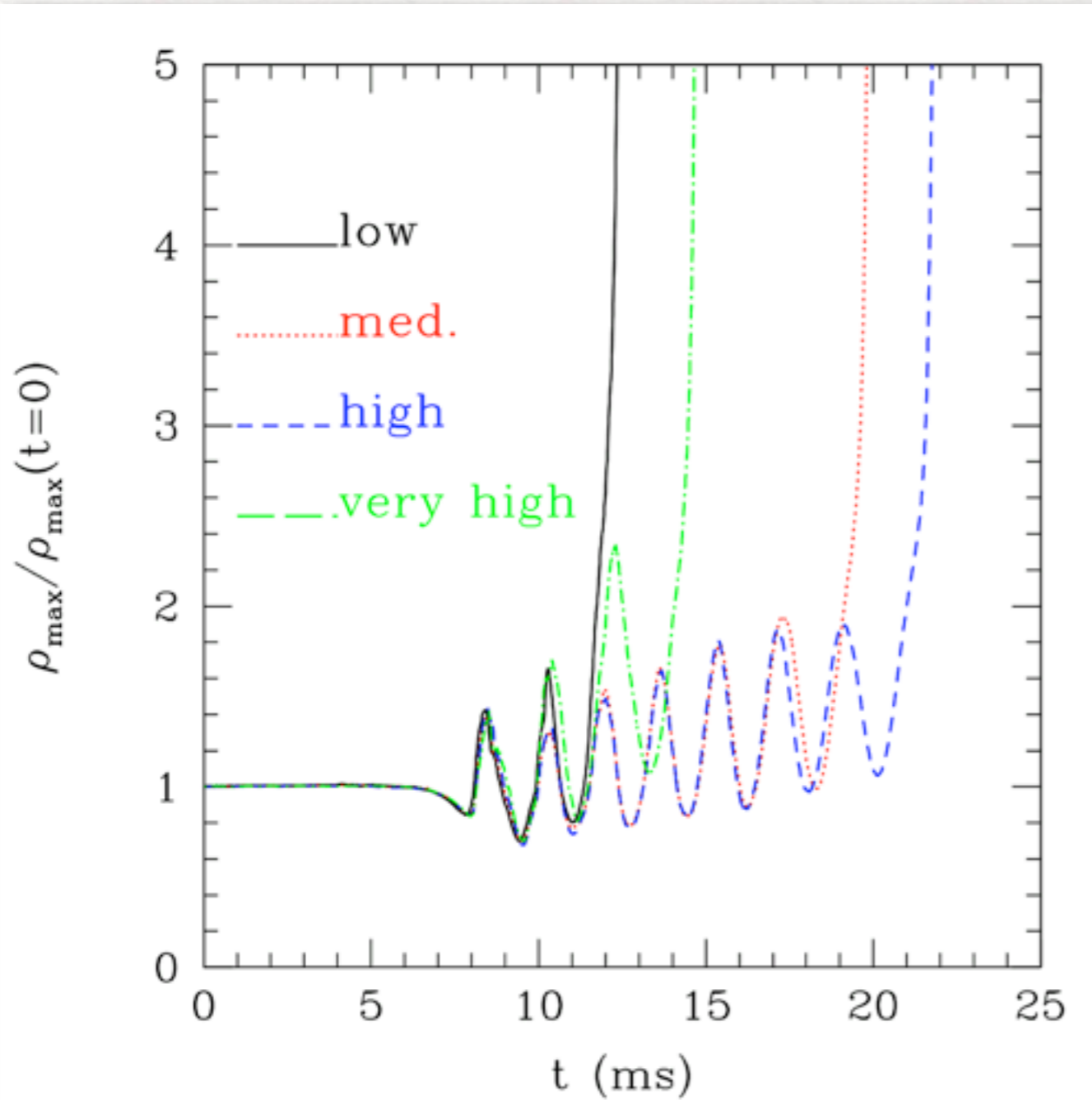
The inspiral seems identical but the postmerger evolution can be rather different. The delay time increases with resolution?...

# Postmerger nightmares..



The inspiral seems identical but the postmerger evolution can be rather different. The delay time increases with resolution?...

# Postmerger nightmares..

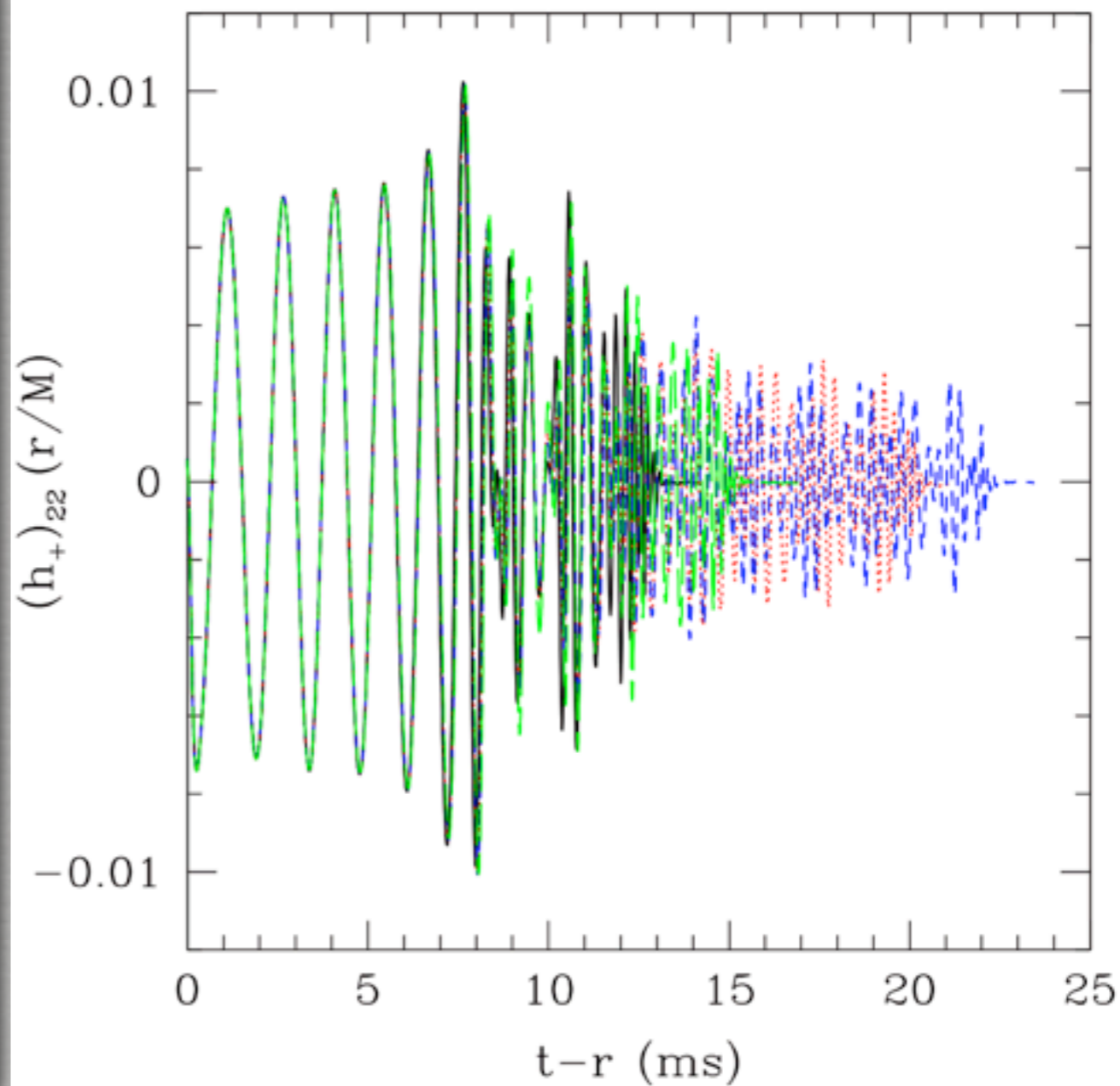
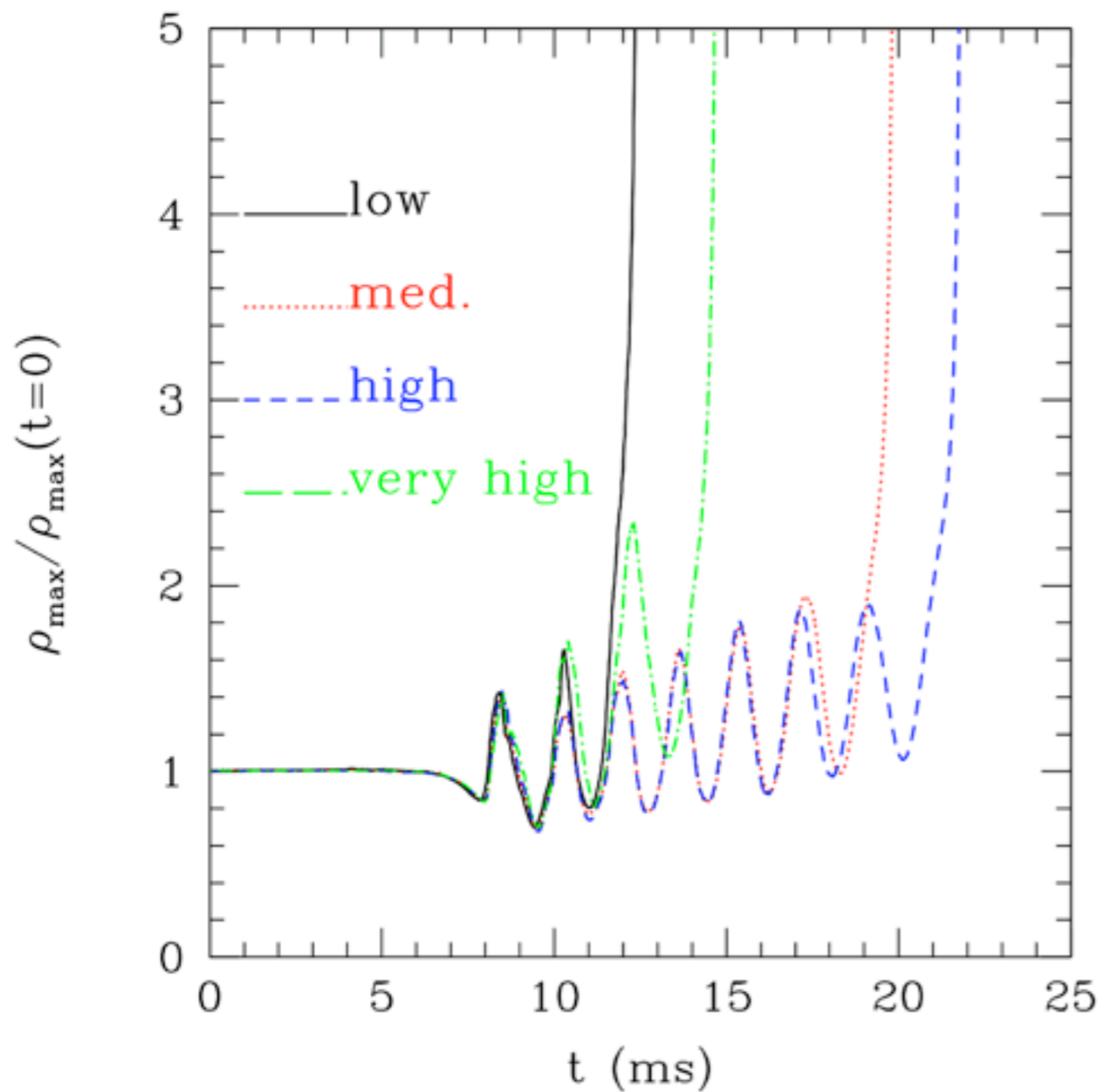


$h = 0.1875 M_{\odot} = 277 \text{ m} : \text{ "low"}$   
 $h = 0.1500 M_{\odot} = 222 \text{ m} : \text{ "med"}$   
 $h = 0.1200 M_{\odot} = 177 \text{ m} : \text{ "high"}$   
 $h = 0.0900 M_{\odot} = 133 \text{ m} : \text{ "very high"}$

The inspiral seems identical but the postmerger evolution can be rather different. The delay time increases with resolution?...

Only to decrease at very high res!

# Postmerger nightmares..

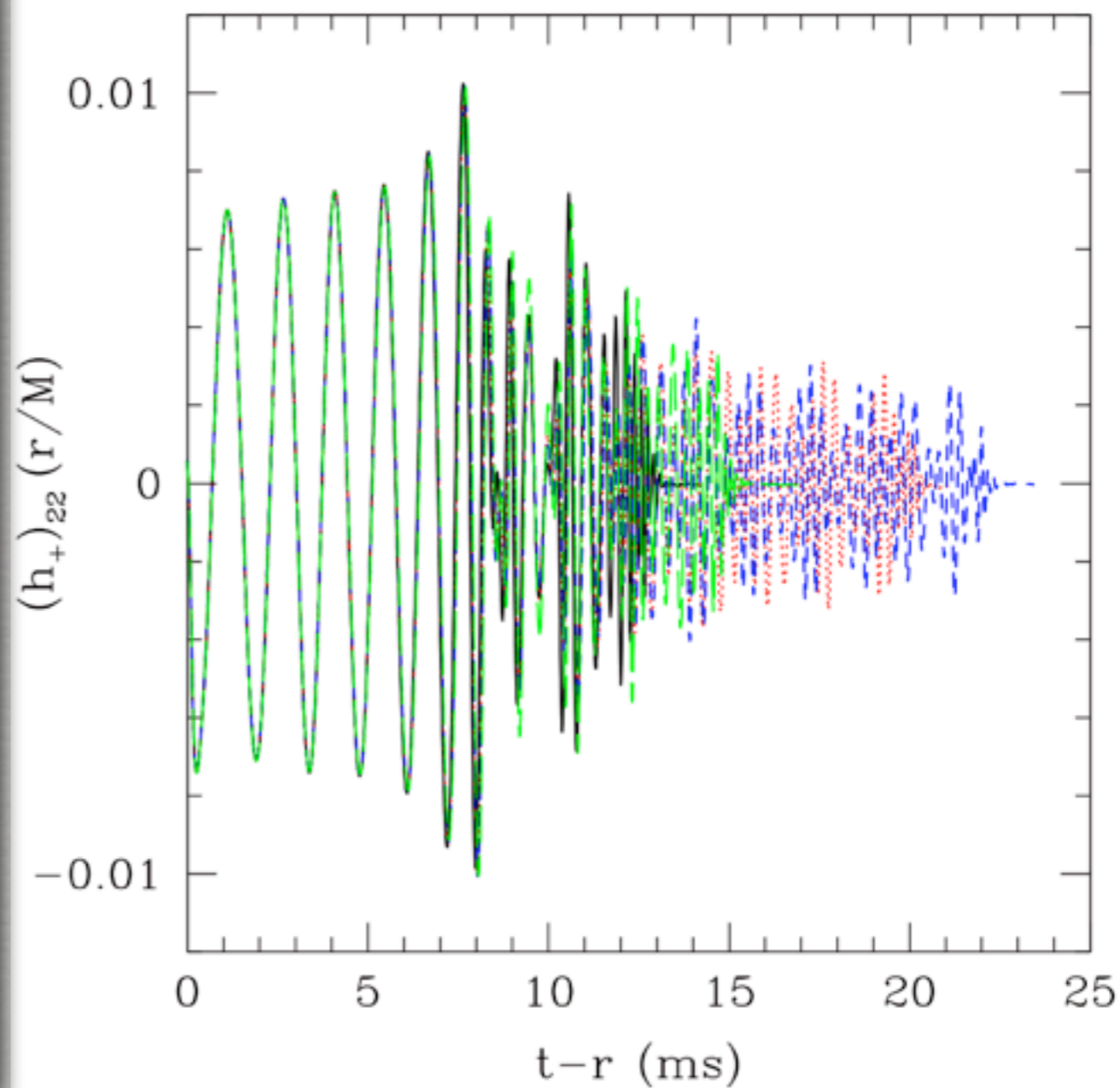
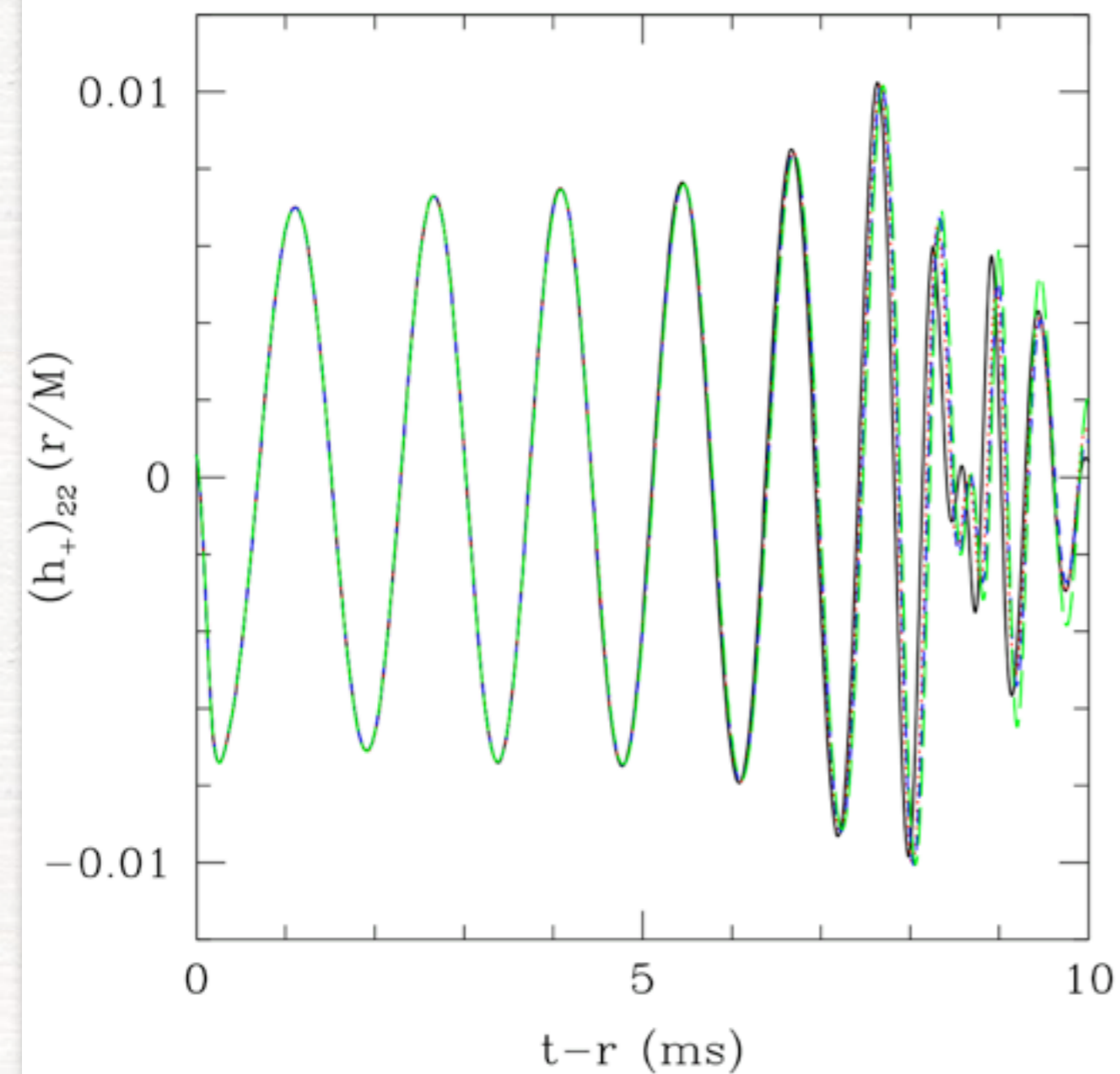


The inspiral seems identical but the postmerger evolution can be rather different. The delay time increases with resolution?...

Only to decrease at very high res!

Of course the same is true also when looking at the GWs..

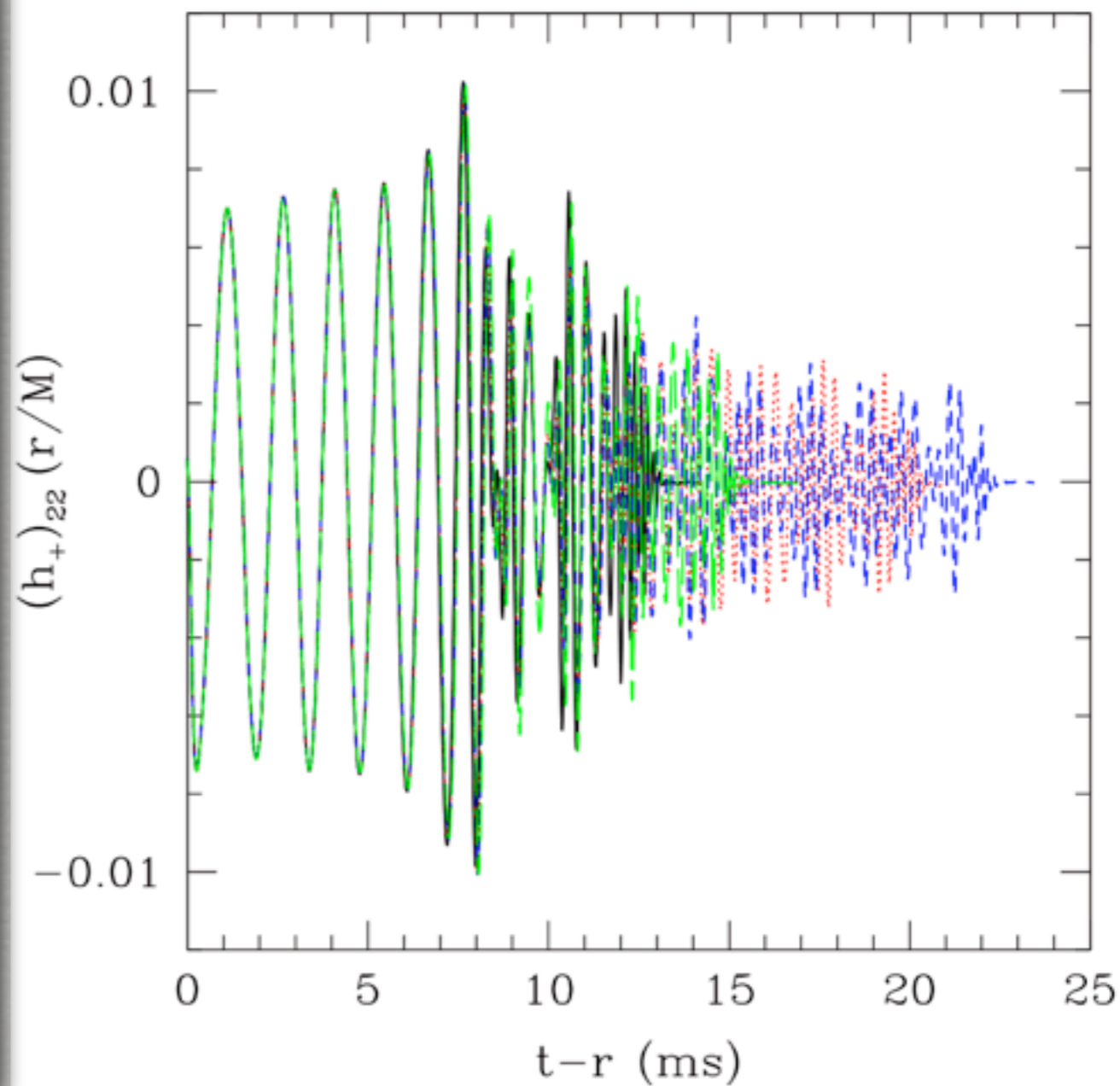
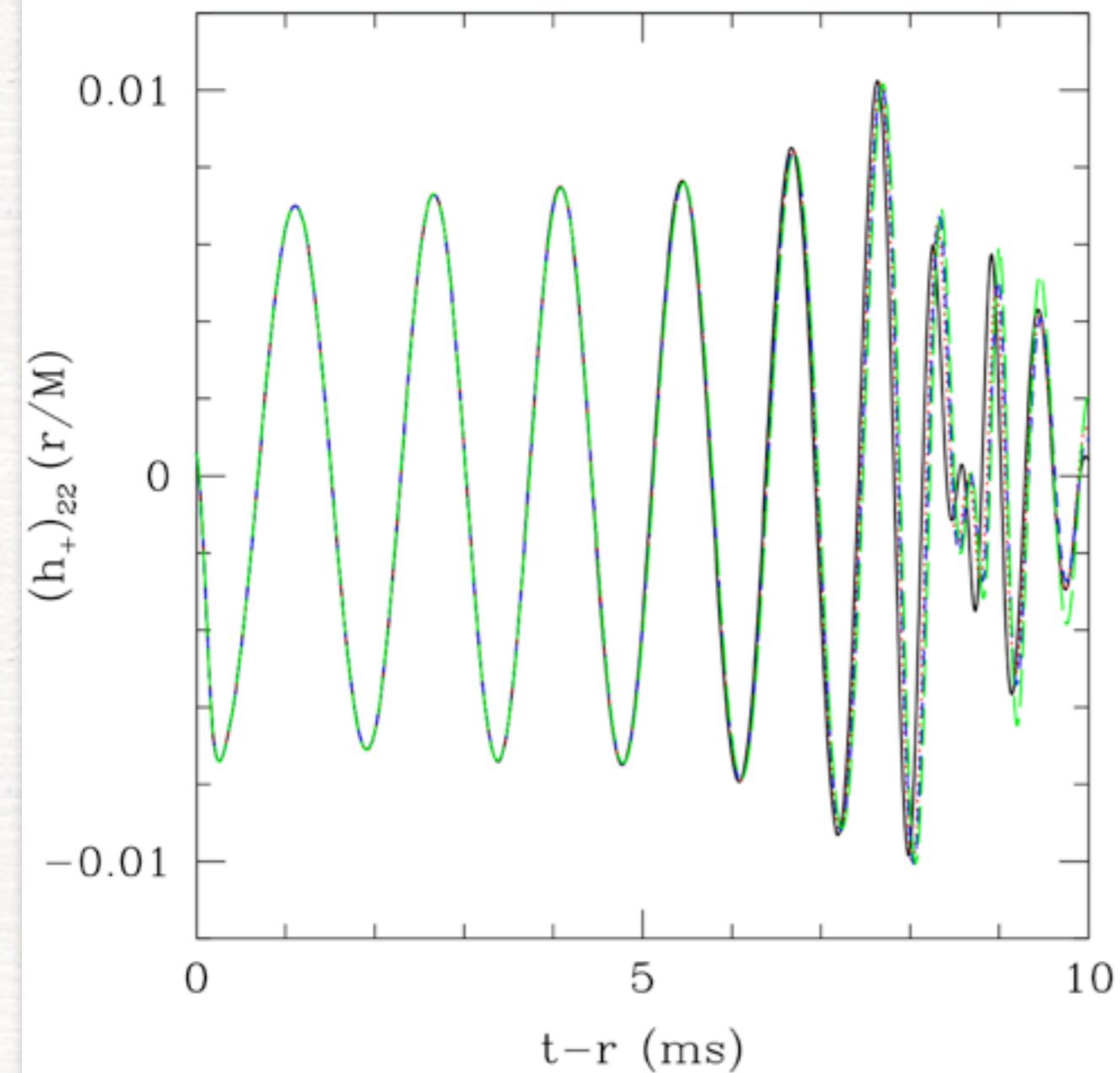
# Postmerger nightmares..



The inspiral is really identical as it is the first few postmerger oscillations.

**Is this a signature that turbulence is responsible for the different behaviour?**

# Postmerger nightmares..



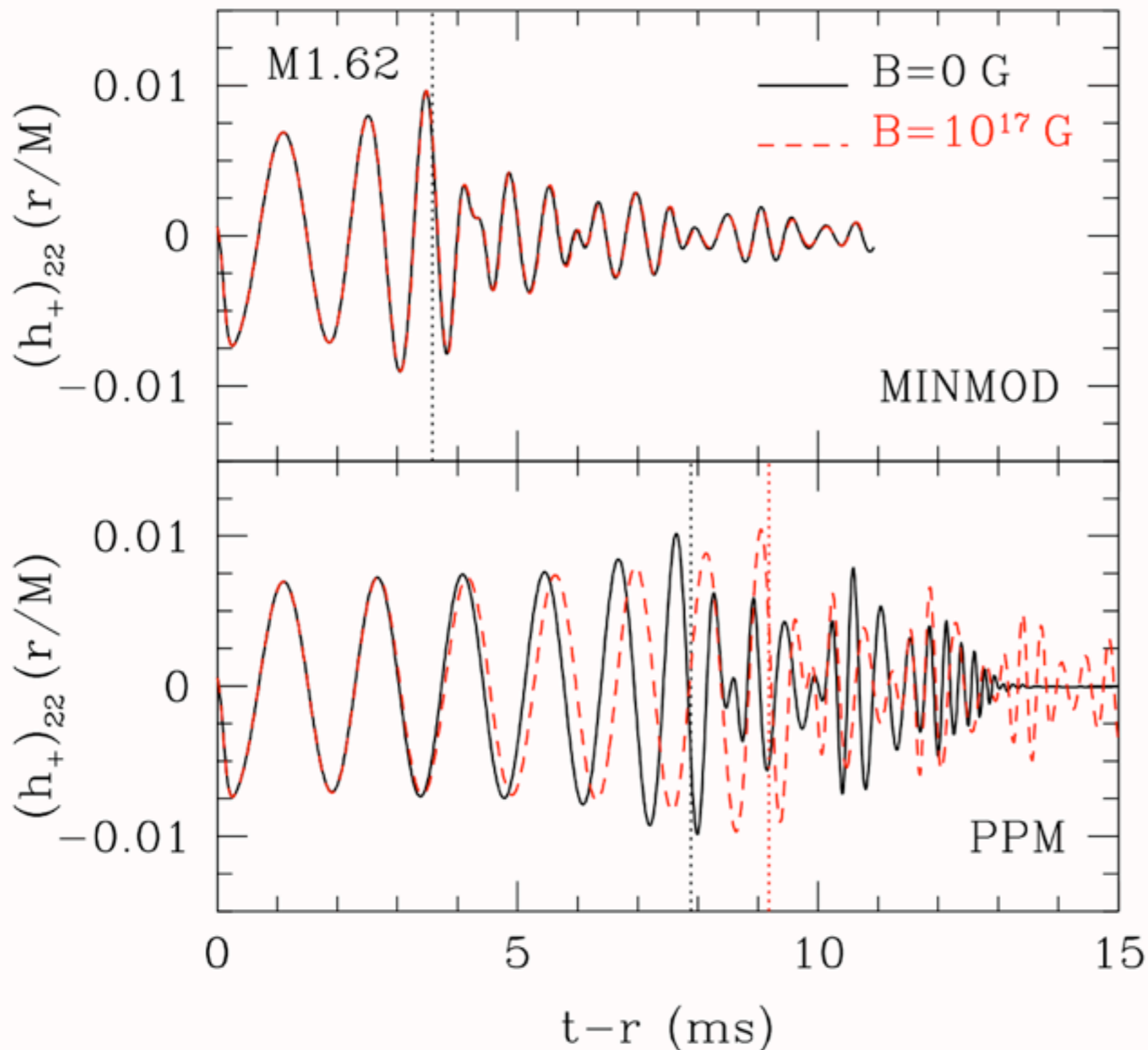
The inspiral is really identical as it is the first few postmerger oscillations.

Is this a signature that turbulence is responsible for the different behaviour?

If this behaviour is generic, it needs to be fully understood before going to finer details on the microphysics...



# Why high-order methods are needed...



Top panel: results obtained using HLLC Riemann solver and a “**minmod**” reconstruction (**2nd-order**)

Bottom results obtained using HLLC Riemann solver and **PPM** reconstruction (**3rd-order**).

Differences are present both during the inspiral and after the merger!

The need for high-order methods and high resolution is **essential**

# Conclusions I

- \* Huge progress has been made in the simulation of compact binaries over the last 4 years (more of this in Shibata, Duez, Neilsen's talks).
- \* With idealized EOSs we have a complete "picture" of BNSs: inspiral, merger, collapse to BH. We can draw this "picture" **with** and **without** magnetic fields, for **equal** and **unequal-mass** binaries.
- \* Astrophysical magnetic fields are unlikely to be strong enough to be detected during the inspiral. However, they will play a role after the merger when amplified by dynamos or instabilities
- \* The dynamics of the postmerger torus is strongly influenced by the presence of magnetic fields and may lead to the launching of a jet. Better handling div-B is necessary for robust modelling

# Conclusions II

- \* While the modelling of the inspiral is robust and without major surprises, the postmerger phase is less robust.
- \* The physics of the merged object is extremely complex and delicate; the degradation of the convergence order doesn't help.
- \* It is possible that realistic EOSs or higher resolutions will remove these difficulties and work is in progress to assess this.
- \* It is also possible that new techniques (eg large-eddy approx.) will be needed; precise timing in GW physics is essential
- \* Much remains to be done to model **realistically** BNSs, both from a **microphysical** point of view (EOS, neutrino emission, etc) and a from a **macrophysical** one (large scale instabilities, etc.).  
More on this in Micra2019...